JOURNAL OF GEOPHYSICAL RESEARCH, VOL. 114, E09003, doi:10.1029/2008JE003244, 2009

An analysis of sinuous ridges in the southern Argyre Planitia, Mars using HiRISE and CTX images and MOLA data

Maria E. Banks,[1] Nicholas P. Lang,[2] Jeffrey S. Kargel,[3] Alfred S. McEwen,[4] Victor R. Baker,[3] John A. Grant,[5] Jon D. Pelletier,[1] and Robert G. Strom[4]

Received 28 July 2008; revised 11 February 2009; accepted 14 May 2009; published 15 September 2009.

[1] A suite of sinuous ridges with branching and braided morphologies forms an anastomosing network in southern Argyre Planitia, Mars. Several modes of origin have been proposed for the Argyre ridges. Imagery from the High Resolution Imaging Science Experiment (HiRISE) and Context Camera (CTX) aboard Mars Reconnaissance Orbiter (MRO) and Mars Orbiter Laser Altimeter (MOLA) topographic data sets from Mars Global Surveyor (MGS) are used to constrain processes involved in formation of the Argyre ridges. We find the characteristics of the ridges and associated layered deposits consistent with glaciofluvial-lacustrine processes and conclude that the ridges are most likely eskers. In particular, variations in ridge height appear to be related to the surrounding surface slope; ridge height increases with descending slopes and decreases with ascending slopes. This characteristic is observed in terrestrial eskers and is related to subice flow processes. The nature of some eroding beds in the ridges suggests induration. If the Argyre ridges are indeed eskers, the southern Argyre basin was once covered by the margin of a large, thick, stagnating or retreating ice deposit that extended for hundreds of kilometers or more. During ridge formation, water flowed on top, within, or beneath the ice deposit; the continuity and preservation of the ridges suggests that flow was primarily at the base of the ice. The dimensions (up to hundreds of meters tall and several kilometers wide), aspect ratio, and extent (hundreds of kilometers) of the ridges, as well as preliminary calculations of discharge, suggest that a significant amount of water was available.

Citation: Banks, M. E., N. P. Lang, J. S. Kargel, A. S. McEwen, V. R. Baker, J. A. Grant, J. D. Pelletier, and R. G. Strom (2009), An analysis of sinuous ridges in the southern Argyre Planitia, Mars using HiRISE and CTX images and MOLA data, *J. Geophys. Res.*, *114*, E09003, doi:10.1029/2008JE003244.

1. Introduction

[2] Argyre Planitia is located within one of the most prominent impact basins on Mars. The Argyre impact basin has a diameter in excess of 1500 km and is located in the southern hemisphere of Mars centered at 50°S and 316°E (http://planetarynames.wr.usgs.gov; Figure 1). The basin is surrounded by mountainous ring ranges: Charitum Montes on the basin's southern side and Nereidum Montes on the basin's northern side. This region appears to have been heavily modified by multiple processes since the formation of the Argyre impact structure leading to many differing interpretations of the geological history of the region. *Hodges* [1980] interpreted the Argyre basin to be modified primarily by large-scale erosion and deposition associated with eolian processes, with possible fluvial and glacial processes playing a minor role. In their geologic map of the Argyre region, *Scott and Tanaka* [1986] proposed significant volcanic activity and deep erosion from wind, periglacial, and fluvial processes. According to *Jöns* [1987, 1999], large portions of the Argyre Planitia have been modified by extensive mud deposits due to melting of the south polar cap. Several studies have interpreted major landforms in the Argyre Planitia and the Charitum Montes as the products of glacial erosional and depositional processes [e.g., *Kargel and Strom*, 1992; *Metzger*, 1991, 1992; *Baker*, 2001; *Hiesinger and Head*, 2002; *Kargel*, 2004; *Banks et al.*, 2007, 2008]. *Parker* [1996a, 1996b] proposed erosional enhancement of the Argyre basin from mass wasting, eolian, fluvial, and lacustrine processes, and suggested that much material in the Charitum and Nereidum Montes has been removed, possibly by fluvial and lacustrine erosion. Layered deposits on the floor of the Argyre basin support hypotheses of a large lake in the basin fed with water which entered the basin through three main large valley networks, Surius, Dzigai, and Pallacopas Vallis (Figure 1b) [e.g., *Kargel and Strom*,

[1]Department of Geosciences, University of Arizona, Tucson, Arizona, USA.
[2]Department of Geology, Mercyhurst College, Erie, Pennsylvania, USA.
[3]Department of Hydrology and Water Resources, University of Arizona, Tucson, Arizona, USA.
[4]Lunar and Planetary Laboratory, University of Arizona, Tucson, Arizona, USA.
[5]Center for Earth and Planetary Studies, National Air and Space Museum, Smithsonian Institution, Washington, D. C., USA.

0148-0227/09/2008JE003244$09.00

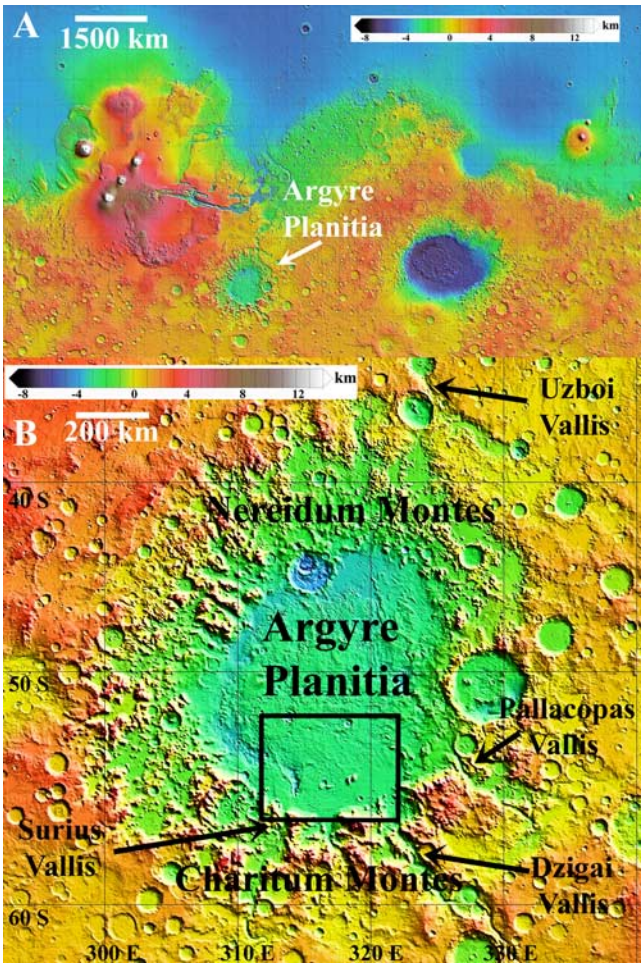

Figure 1. Location of the study area. (a) MOLA shaded relief map of Mars (http://mola.gsfc.nasa.gov/images.html) showing the location of Argyre Planitia in the southern hemisphere (centered at 50°S and 316°E). (b) Close-up view of Argyre Planitia. The black outline indicates the general location of the sinuous ridges on the basin floor and the location of Figure 2.

1992; *Parker*, 1989, 1994; *Parker et al.*, 2000, 2003; *Kargel*, 2004], possibly originating as meltwater from a Hesperian aged melting of the south polar cap [*Head*, 2000a, 2000b, 2000c; *Head and Pratt*, 2001].

[3] A suite of ridges with sinuous, branching, and braided morphologies forms an anastomosing network around the southern edge of the Argyre basin (Figure 2). Owing to the complex geological history of the Argyre region, several formation mechanisms have been proposed for the sinuous ridges. For example, the Argyre ridges have been interpreted as wrinkle ridges [*Tanaka and Scott*, 1987], exhumed igneous [*Carr and Evans*, 1980] and clastic [*Ruff and Greeley*, 1990] dikes, lava flow features [*Tanaka and Scott*, 1987], linear sand dunes [*Parker et al.*, 1986; *Ruff and Greeley*, 1990; *Ruff*, 1992], lacustrine spits or barrier bars [e.g., *Parker et al.*, 1986; *Parker and Gorsline*, 1992; *Parker*, 1994, 1996a, 1996b], glacial moraines [*Hiesinger and Head*, 2002; *Kargel*, 2004], inverted stream topography [*Howard*, 1981], frozen waves in a large-scale mudflow [*Jöns*, 1992], and eskers or infilled river channels formed from meltwater flowing on top, within, or beneath a large ice mass [e.g., *Carr and Evans*, 1980; *Howard*, 1981; *Ruff and Greeley*, 1990; *Metzger*, 1991, 1992; *Kargel and Strom*, 1992; *Hiesinger and Head*, 2002; *Kargel*, 2004; *Lang*, 2007]. Understanding the origin of the Argyre ridges is important because it provides insight into the geological history of this region and perhaps the global history of water on Mars. Analysis of similar sinuous ridges in the Dorsa Argentea Formation, near the south pole of Mars, has led several workers to conclude that the Dorsa Argentea ridges are eskers [e.g., *Kargel*, 1993; *Head*, 2000a, 2000b; *Head and Hallet*, 2001a, 2001b; *Head and Pratt*, 2001; *Ghatan and Head*, 2004]. This hypothesis has important climatic implications as eskers are associated with water flows under or within large ice deposits, and their presence suggests past glaciations on Mars. On the basis of their similarities to terrestrial eskers, the Argyre sinuous ridges have also been interpreted as Martian eskers [e.g., *Howard*, 1981; *Ruff and Greeley*, 1990; *Metzger*, 1991, 1992; *Kargel and Strom*, 1992; *Hiesinger and Head*, 2002; *Kargel*, 2004; *Lang*, 2007], but this interpretation remains controversial.

[4] Images with a scale as small as 0.25 m/pixel from the HiRISE camera aboard MRO, are revealing previously undiscerned details of the Martian surface [*McEwen et al.*, 2007]. Here we use HiRISE and CTX imagery (pixel scale of 6 m/pixel) and MOLA topographic data sets [*Smith et al.*, 2001] to characterize the Argyre sinuous ridges more definitively, and to further constrain the processes involved in their formation. We review past Argyre sinuous ridge research and reassess several of the proposed formation hypotheses, focusing specifically on linear sand dunes, lava flow features, exhumed igneous dikes, wrinkle ridges, lacustrine spits and barrier bars, glacial moraines and crevasse fill ridges, inverted streams, and eskers, using characteristics of the ridges from observations discussed in previous literature and confirmed here with HiRISE, CTX, and MOLA data, as well as several new observations. Topographic analyses of the Argyre sinuous ridges were previously completed by *Hiesinger and Head* [2002], who looked at one main ridge, and *Lang* [2007]. Here we take an in depth look at the morphology of the ridges and their relationship to the surrounding terrain, and extend our topographic analysis to include multiple ridges to determine whether they consistently exhibit the same characteristics. We conclude that the characteristics of the ridges are most consistent with terrestrial subice fluvial processes, and that the ridges are most likely eskers. On the basis of this interpretation, details revealed in HiRISE and CTX imagery and MOLA data are used to investigate the environment in which the ridges formed.

2. Sinuous Ridge Characteristics

[5] In planform, the Argyre sinuous ridges vary from solitary sinuous ridges with an average sinuosity of ~1.2 [*Kargel*, 1993], to branching and braided patterns of ridges (Figures 2 and 3). Although they are primarily solitary sinuous forms, some sections of the ridges exhibit complex braided patterns, low and high tributary junction angles, and confluent and diffluent branches (Figures 2 and 3). Ridges have also been diverted around large obstacles such as the

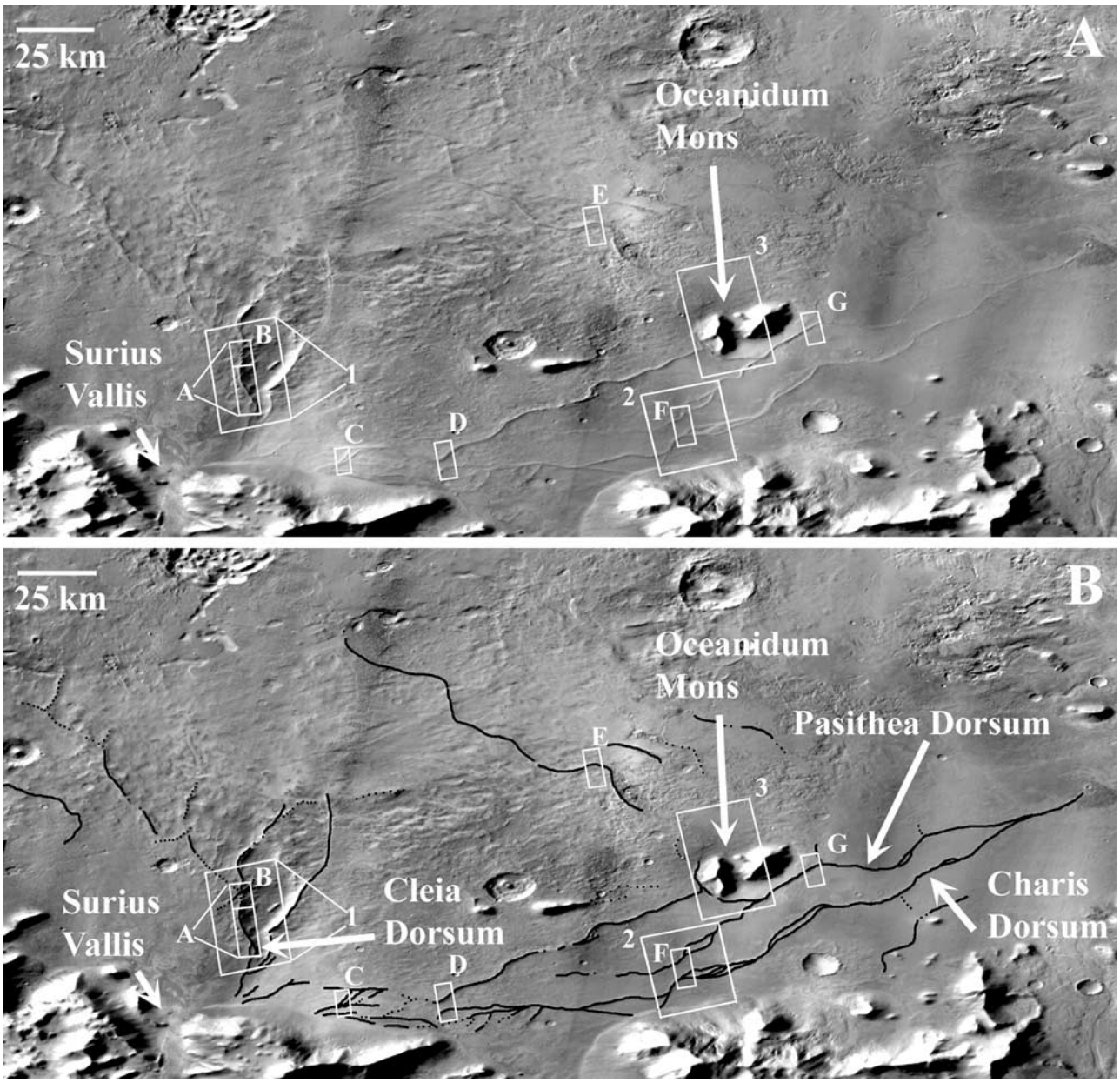

Figure 2. (a) Mars Odyssey Thermal Emission Imaging System (THEMIS) daytime IR mosaic (http://jmars.asu.edu) of the southern Argyre basin (Figure 1). A suite of sinuous ridges with branching and braided morphologies forms an anastomosing network in this portion of the basin. Lettered white outlines mark the approximate footprints of HiRISE images discussed in this study: image A, PSP_001904_1245; image B, PSP_003816_1245 and PSP_004106_1245; image C, PSP_003183_1235; image D, PSP_007007_1235; image E, PSP_006875_1255; image F, PSP_001640_1240; image G, PSP_001508_1245. Numbered white outlines mark the approximate footprints of CTX images discussed in this study: image 1, P02_001904_1244_XI_55S045W_06122; image 2, P02_001640_1240_XI_56S041W_061202; image 3, P03_002339_1249_XI_55S041W_070125. (b) Blacks lines have been added to the mosaic from Figure 2a to mark the locations of sinuous ridges. The three main ridges discussed in this study are labeled: Cleia, Pasithea, and Charis Dorsum.

massif Oceanidum Mons (Figures 2 and 3b). HiRISE and CTX images show ridge crests ranging from smooth, curved surfaces to flat-topped, relatively sharp crested (inverted v), or multiple crested forms (Figure 4). Cross-sectional profiles derived from MOLA Precision Experiment Data Records (PEDRs) (available at http://pds-geosciences.wustl.edu/missions/mgs/pedr.html) confirm ridge crest shapes and show that ridges also vary in symmetry along their extent (Figure 5). Width and height vary along the length of each ridge as well; widths typically range from ~1 to 4 km and heights typically range from ~10 to 300 m (Figure 5). Although each ridge consists of several discontinuous segments ranging in length from less than 1 km to more than 120 km, the ridges have a high continuity (the ratio

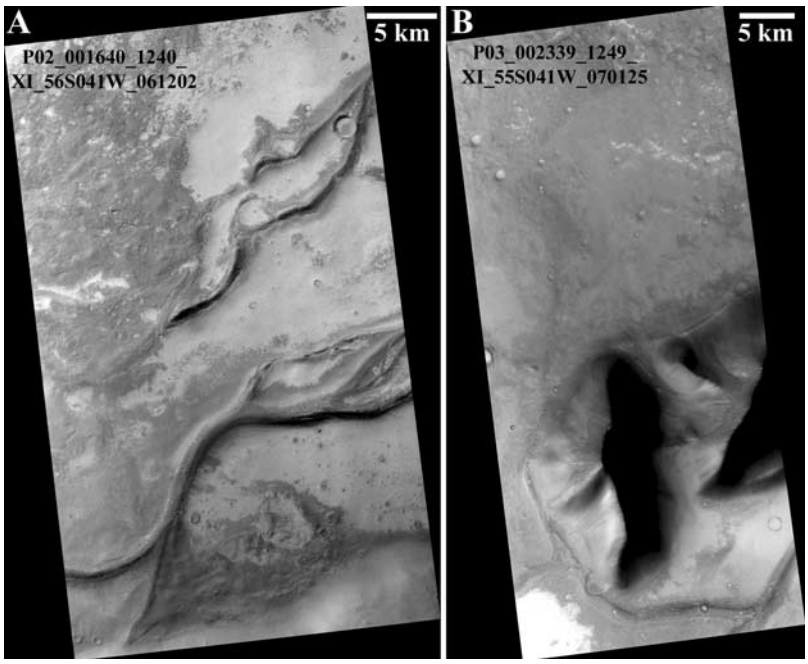

Figure 3. Although they are primarily solitary sinuous forms, some sections of the Argyre sinuous ridges exhibit complex braided and branching patterns. (a) CTX image P02_001640_1240_XI_56S041W_061202 shows details in the planform patterns of Argyre sinuous ridges. (b) The ridges appear to divert around large obstacles such as the massif, Oceanidum Mons, seen here in CTX image P03_002339_1249_XI_55S041W_070125.

of the length of an individual ridge segment to the total length of a series of ridge segments) of approximately 97% [*Metzger*, 1992].

[6] Layers or beds are observed in portions of several ridges (Figure 6) [e.g., *Parker et al.*, 1986; *Hiesinger and Head*, 2002; *Kargel*, 2004; *Lang*, 2007]. In some locations layers are laterally continuous for several kilometers (Figure 6b), while in others the layers appear to be discontinuous and pinch out (Figure 6c). In close-up views from HiRISE images, layers of material more resistant to erosion, possibly indurated material, appear to alternate with more easily eroded layers (Figure 6c). In at least two locations, layers observed on either side of a ridge and can be traced across the width of the ridge (Figures 6d and 6e). A 1 m/post digital elevation model (DEM) showing a portion of Cleia Dorsum (Figure 7), was produced from a stereo pair of HiRISE images. The DEM was created using the area-based automatic matching package of the commercial stereo software SOCET SET (®BAE Systems) and a preprocessing method developed by *Kirk et al.* [2008]. The vertical precision of the DEM is ~20 cm [*Kirk et al.*, 2008]. Cross-sectional profiles of Cleia Dorsum, acquired from the DEM, show that individual layers occur within ~1 m of the same elevation on both sides of the ridge (Figure 7g). Profiles tracing layers along the length of the ridge show that the layers have slight undulations and slopes but, at least in this portion of this ridge, are essentially horizontal (Figure 7h). In the same section of Cleia Dorsum, layers in the lower portion and on the western side of the ridge extend into the surrounding topography (Figure 8a). Layers extending from the ridges into the surrounding topography in southern Argyre were also observed and discussed by *Parker* [1994] and *Parker et al.* [1986]. However, this continuity of layering is

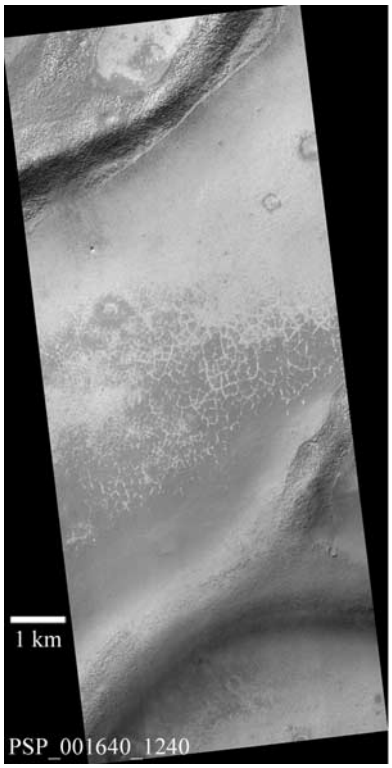

Figure 4. Variations in the shape of ridge crests can be clearly seen in HiRISE images. In the upper ridge, the crest varies from a smooth curved surface to a more relatively sharp crested shape. The lower ridge exhibits both smooth, curved surfaces and multicrested forms (HiRISE image PSP_001640_1240).

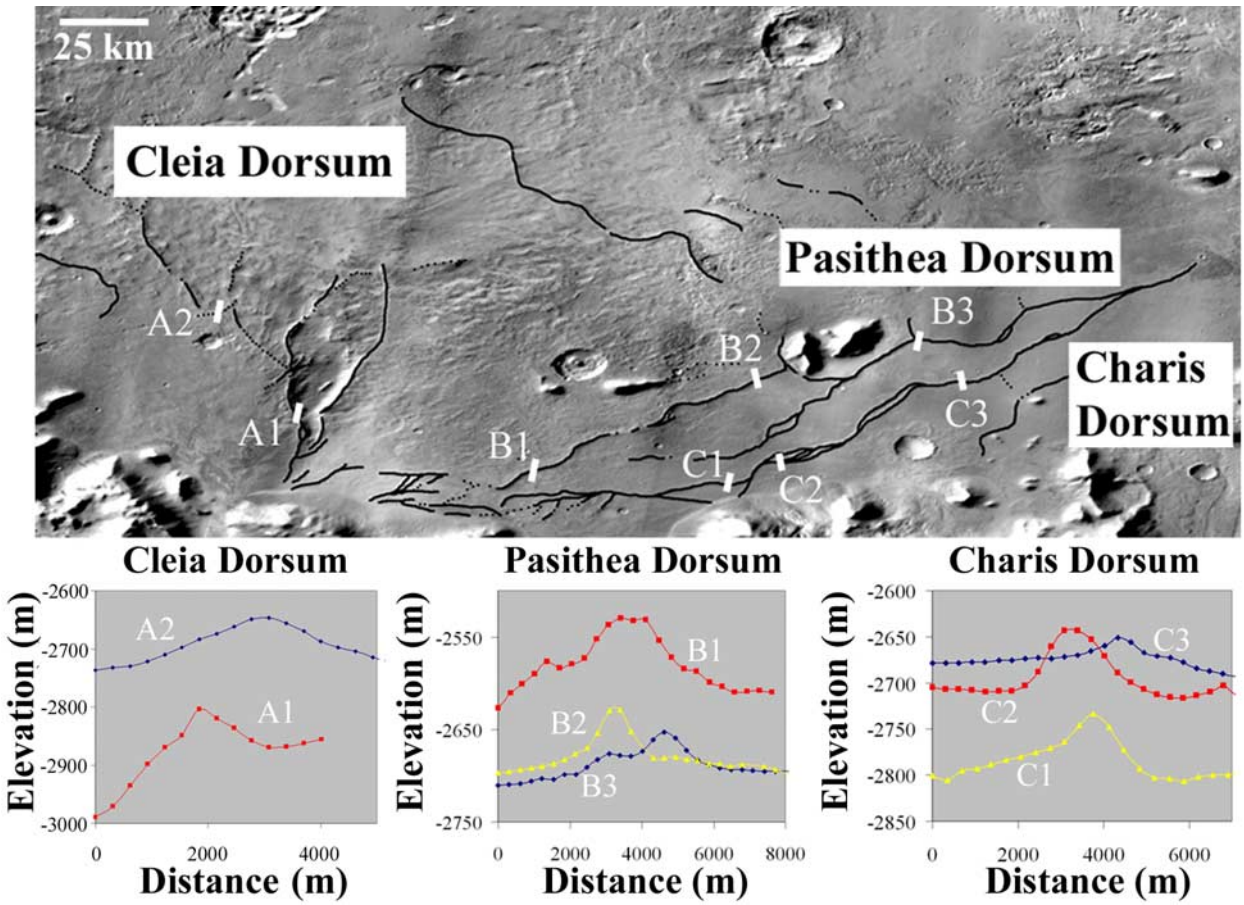

Figure 5. Cross-sectional profiles from three Argyre sinuous ridges derived from MOLA PEDR tracks. Sinuous ridges are outlined in black on a THEMIS daytime IR mosaic (http://jmars.asu.edu). The locations of profiles are indicated with white lines on the ridges. Plots of cross-sectional profiles show that ridges vary in symmetry along their extent and that ridge crests range in shape from smooth, curved surfaces to flat-topped, relatively sharp crested (inverted v), or multiple crested forms. Profiles often show offsets in the elevation of the surrounding surface (sometimes over 50 m) on either side of the ridges. Width and height also vary along the length of each ridge with widths of up to several kilometers and heights of up to hundreds of meters.

observed in only portions of the Argyre ridges. Also observed in this part of Cleia Dorsum (where it trends in a northwesterly direction) is a secondary ridge that cross-cuts the main ridge and trends in a northeasterly direction (Figure 8). Large, U-shaped grooves have been carved into the secondary ridge (Figure 8d).

[7] HiRISE images resolve large boulders, some greater than 8 m in scale, in layers and on the surfaces of ridges (Figure 9). The boulders tend to be angular in shape and are generally not observed in the same abundance on the surrounding terrain. Close-up views of ridge surfaces and layers reveal that many of the large boulders, particularly angular ones, appear to be interlocking and form geometric patterns. This suggests that these are not discrete boulders that were transported, but rather are a lag produced by fracturing and erosion of indurated or cemented layers of smaller, relatively fine-grained material. Most likely, predominantly gravel to sand sized sediments, or smaller, were transported and deposited in the ridges. The sediments appear to have become indurated through secondary processes, and have subsequently fractured and eroded into boulder sized material. Whether some of the large boulders may have been transported, perhaps those that are more rounded, is unclear.

[8] In several locations, sinuous ridges lie within a shallow trough (Figure 10). Troughs appear to be mantled with finer sediments and can extend laterally for several kilometers. MOLA data reveal that some troughs are more than 10 m in depth below the elevation of the surrounding surface. Only portions of some of the Argyre ridges are observed in troughs.

[9] A topographic analysis of the Argyre sinuous ridges was completed using three main ridges: Cleia Dorsum, Pasithea Dorsum, and Charis Dorsum (Figure 11). These ridges were chosen because they have been imaged most extensively by HiRISE (Figure 2). Multiple cross-sectional profiles were derived from MOLA PEDR tracks along the extent of the three ridges. The cross-sectional profiles show that in several locations the adjacent surface elevation differs, sometimes by tens of meters, on either side of the ridges suggesting that ridges may be oriented across slopes rather than consistently downslope (Figure 5). The elevation of the surrounding surface was then averaged at each profile location and plotted as a function of distance along the

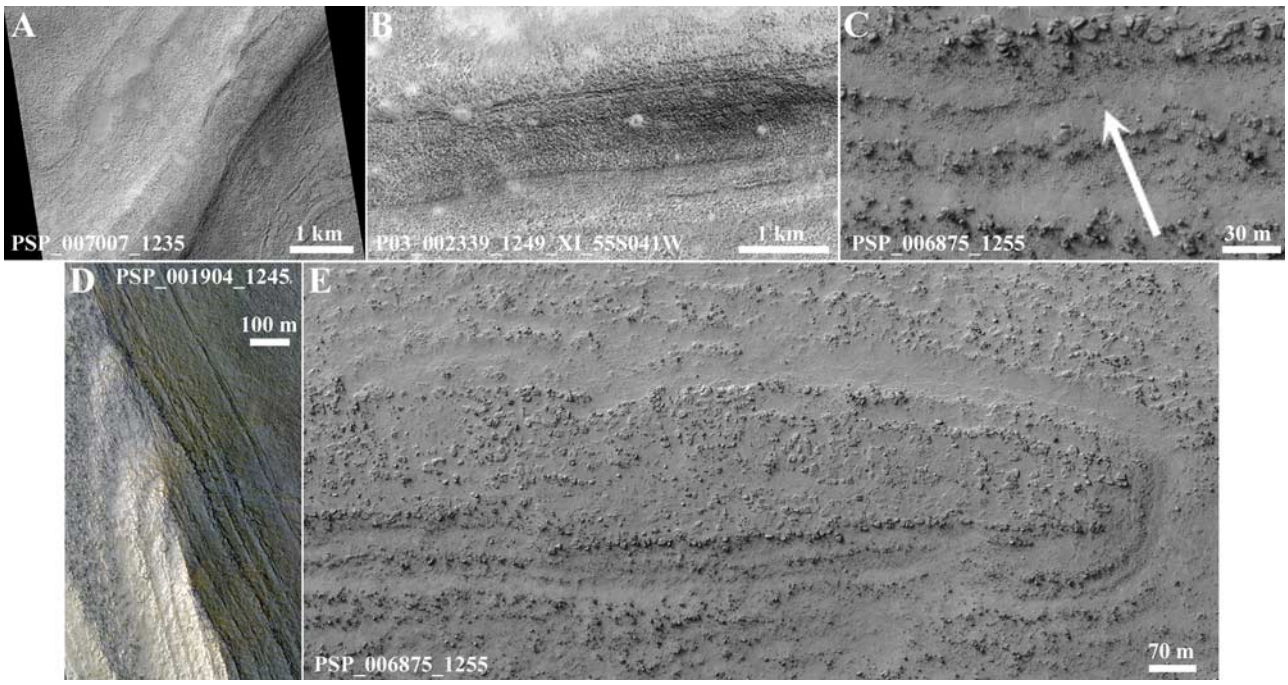

Figure 6. Examples of layering in Argyre sinuous ridges. (a) Layering in Pasithea Dorsum seen in HiRISE image PSP_007007_1235. (b) CTX image P03_002339_1249_XI_55S041W_070125 shows layers that are continuous for several kilometers. (c) A close-up view of the ridge in HiRISE image PSP_006875_1255 reveals layers of material resistant to erosion, perhaps indurated sediments, alternating with less resistant layers. One of the layers visible in the left side of the image appears to pinch out (white arrow), although the apparent pinching out could be due to mantling. Layers can be traced across the width of ridges in (d) HiRISE false color image PSP_001904_1245 and (e) HiRISE image PSP_006875_1255.

extent of each ridge (Figure 11b). For each of the ridges, the overall elevation at which they occur varies along trend with a difference between the maximum and minimum elevation of the surrounding surface of ~110 m for Pasithea and Charis Dorsum, and ~200 m for Cleia Dorsum (the surrounding surface exhibits slopes of up to ~5° along the length of the ridges); this suggests that the Argyre sinuous ridges cross topography. The elevation of the ridge crest in each MOLA track was then measured and plotted as a function of distance along the same three ridges revealing that the height of each ridge also varies along its extent; the difference between the maximum and minimum height for the ridges is ~95 m for Pasithea and Charis Dorsum, and ~260 m for Cleia Dorsum (Figure 11b). To understand the relationship of ridge height to the surrounding terrain, the change in ridge height between successive MOLA tracks was plotted against the slope of the surrounding surface along the length of each ridge (Figure 11c). For slopes greater than 1°, ridge height increases with descending slopes and decreases with ascending slopes. Further analysis of cross-sectional profiles also reveals that ridges tend to have sharper crested shapes on descending and flat slopes, and low, broad, and more rounded shapes on ascending slopes.

[10] MOLA PEDR tracks were used for the topographic analysis owing to their coverage along the full extent of the ridges. At the time of this writing, the limited number of HiRISE and CTX stereo pairs in the southern Argyre basin provided insufficient coverage for a large-scale topographic analysis. A comparison of MOLA PEDR tracks with profiles acquired from the HiRISE DEM (Figure 7f) showed that elevations from both data sets differed by a maximum of ~10 m and usually differed by only a few meters (Figure 7i).

3. Discussion

[11] Argyre sinuous ridges have been interpreted as linear sand dunes [*Parker et al.*, 1986; *Ruff and Greeley*, 1990; *Ruff*, 1992], lava flows features [*Tanaka and Scott*, 1987], exhumed igneous dikes [*Carr and Evans*, 1980], wrinkle ridges [*Tanaka and Scott*, 1987], lacustrine spits and barrier bars [e.g., *Parker et al.*, 1986; *Parker and Gorsline*, 1992; *Parker*, 1994, 1996a, 1996b], glacial moraines [*Hiesinger and Head*, 2002; *Kargel*, 2004] and crevasse fill ridges, inverted stream topography [*Howard*, 1981], and eskers [e.g., *Carr and Evans*, 1980; *Howard*, 1981; *Parker et al.*, 1986; *Ruff and Greeley*, 1990; *Metzger*, 1991, 1992; *Kargel and Strom*, 1992; *Hiesinger and Head*, 2002; *Kargel*, 2004; *Lang*, 2007]. Here we review past sinuous ridge research and reassess several formation hypotheses using our current understanding of ridge characteristics.

[12] An eolian origin for the Argyre ridges is supported by the appearance of dunes on all geological units associated with the Argyre basin [*Hiesinger and Head*, 2002]. Linear or longitudinal sand dunes exist as elongated, sharp crested ridges that extend parallel to the net wind direction [e.g., *Ritter et al.*, 2002], and are usually separated by a sand

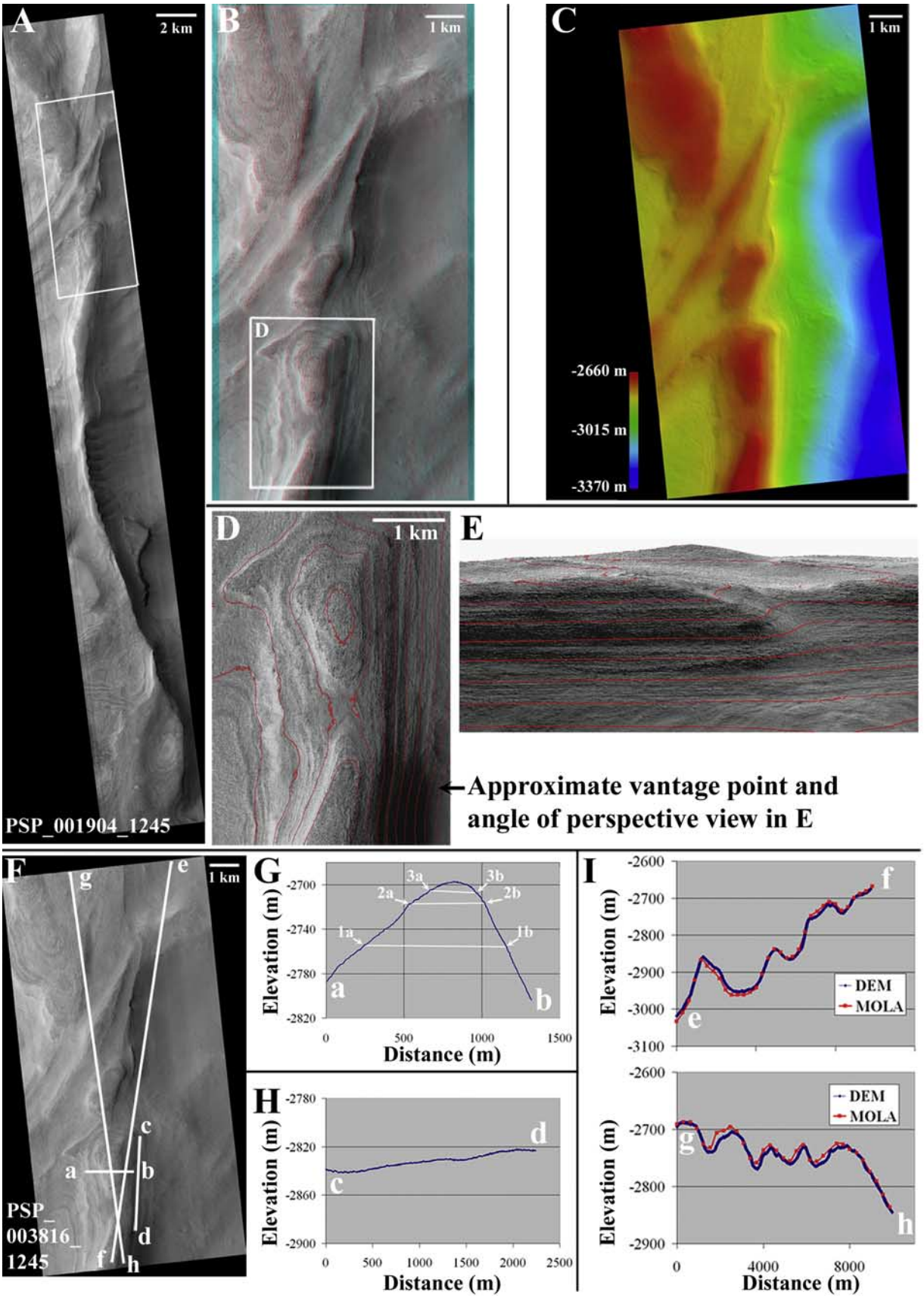
A
2 km
PSP_001904_1245
B
1 km
D
C
1 km
-2660 m
-3015 m
-3370 m
D
1 km
E
Approximate vantage point and angle of perspective view in E
F
1 km
g
e
c
a
b
d
f
h
PSP_003816_1245
G
Elevation (m)
-2700
-2740
-2780
-2820
3a
3b
2a
2b
1a
1b
a
b
0
500
1000
1500
Distance (m)
H
Elevation (m)
-2780
-2820
-2860
-2900
d
c
0
500
1000
1500
2000
2500
Distance (m)
I
Elevation (m)
-2600
-2700
-2800
-2900
-3000
-3100
f
e
DEM
MOLA
Elevation (m)
-2600
-2700
-2800
-2900
g
h
DEM
MOLA
0
4000
8000
Distance (m)

Figure 7

free surrounding surface (Figure 12) [e.g., *Easterbrook*, 1999]. Terrestrial linear sand dunes commonly occur in long parallel chains with regular spacing but, like the Argyre ridges, can be oriented in more than one direction within the same region [*Ritter et al.*, 2002]. Typical terrestrial linear dunes [*Mainguet*, 1984], as well as typical Martian dunes [*Greeley et al.*, 1992], are usually shorter, thinner, and lower in height than the Argyre ridges [*Ruff*, 1992; *Hiesinger and Head*, 2002] and more closely spaced [*Ruff*, 1992; *Ritter et al.*, 2002], but seif dunes, a type of longitudinal dune, can be up to 300 km long and 200 m high [*Easterbrook*, 1999]. While terrestrial linear sand dunes can also be sinuous and bifurcate [*Mabbutt and Sullivan*, 1968], they do not match the higher sinuosity [*Kargel*, 1993] and complex intersecting and bifurcating patterns of the Argyre ridges [*Ruff and Greeley*, 1990]. Although not diagnostic, HiRISE images reveal that Martian dunes usually have ripples superposed on their surface (Figure 12), something not observed on most Argyre ridge surfaces. Linear sand dunes also do not typically occur within troughs. Layers are not commonly observed in Martian sand dunes as well; linear sand dunes would have to erode in a very unusual way to expose layers that appear to be horizontal. Even if layering were exposed in a linear dune, it would not extend into the surrounding topography.

[13] The morphology and braided and branching patterns of the Argyre sinuous ridges vary considerably from typical lava flow–related features such as basaltic pressure ridges or flow lobes [*Theilig*, 1986; *Ruff and Greeley*, 1990; *Head*, 2000a; *Hiesinger and Head*, 2002]. Although the ridges could represent an unusual lava flow feature, *Hiesinger and Head* [2002] inspected MOC images covering the geologic unit on which the Argyre ridges occur and found no evidence for source vents, flow fronts, or other volcanic constructs, making a volcanic origin for the ridges less likely. The braided patterns and sinuosity of the ridges are also atypical of dike propagation patterns suggesting the Argyre ridges are not exhumed igneous dikes [*Pollard*, 1987; *Head et al.*, 2006]. Examples of inclined igneous dikes, such as those in the Karoo Basin in South Africa and the Whin Sill in the UK [e.g., *Goulty and Schofield*, 2008], exhibit similar sinuous forms, but any layering present in these features, in the form of cooling joints, should also be obviously inclined [*Grossenbacher and McDuffie*, 1995] and layering would not be continuous with surrounding plains.

[14] Wrinkle ridges are linear to arcuate positive relief features that have been identified on the Moon, Mars, Mercury, and Venus. Martian wrinkle ridges are typically tens to hundreds of kilometers in length, up to a few kilometers in width, and a few hundred meters in height [*Golombek et al.*, 1991, 2000]. Although the dimensions of the Martian wrinkle ridges and the Argyre sinuous ridges are similar, their cross-sectional profiles generally differ in shape [*Hiesinger and Head*, 2002]. For example, cross-sectional profiles of wrinkle ridges are typically more asymmetric than profiles of the Argyre ridges. Wrinkle ridge profiles also commonly exhibit a superposed hill or smaller, steep ridge on a broad rise or arch (Figure 13) [e.g., *Golombek et al.*, 1991, 2000], something not commonly observed in the Argyre ridge profiles (Figure 5) [*Hiesinger and Head*, 2002]. Cross-sectional profiles of both the Argyre ridges and wrinkle ridges often show offsets in elevation on either side of the ridge. However, offsets in the Argyre examples are smaller, up to ~75 m [*Hiesinger and Head*, 2002], than offsets observed in Martian wrinkle ridges, up to 225 m [*Golombek et al.*, 1991]. Although there is considerable overlap, *Kargel* [1993] found the sinuosity of the Argyre sinuous ridges slightly higher than that of wrinkle ridges [*Hiesinger and Head*, 2002]. Wrinkle ridges also have a much lower lateral continuity, commonly form en echelon patterns [*Golombek et al.*, 1991], and generally occur in more linear and orthogonal patterns in comparison to the braided and branching patterns formed by the Argyre ridges. Wrinkle ridges are most commonly believed to form from horizontal compression or shortening of the crust due to faulting [*Golombek et al.*, 1991, 2000] and thus any layering in the ridges would be tilted. *Hiesinger and Head* [2002] argued that the undisturbed, continuous layering observed in the Argyre ridges is also inconsistent with a tectonic origin. In addition, HiRISE images of wrinkle ridges reveal that these features are not typically observed in troughs and vary from the Argyre ridges in their detailed structure and surface texture (Figure 13).

[15] The association of the ridges with layered plains material on the basin floor, supports the hypothesis that the Argyre ridges represent long spits or bars of channel sediments deposited by wave-generated drift currents in a large shallow lake [e.g., *Parker et al.*, 1986; *Parker and Gorsline*, 1992; *Parker*, 1994, 1996a, 1996b]. Terrestrial spits and bars form by longshore transport of sediment; most form

Figure 7. A 1 m/post DEM, showing a portion of Cleia Dorsum, was created using HiRISE stereo pair PSP_003816_1245 and PSP_004106_1245. The vertical precision of the DEM is ~20 cm [*Kirk et al.*, 2008]. (a) Cleia Dorsum as seen in HiRISE image PSP_001904_1245. The white box marks the location and area covered by the DEM. Different products produced from the DEM (Figures 7b–7e), such as (b) an anaglyph, (c) colorized shaded relief map, (d) contour map (contour interval is 25 m), and (e) perspective view of the contour map, all clearly show that the layers in this portion of the ridge are horizontal or near horizontal. The white box in Figure 7b shows the outline of the contour map in Figure 7d. The black arrow in Figure 7d shows the approximate vantage point and angle of the perspective view in Figure 7e. The perspective view in Figure 7e has 5X vertical exaggeration. (f) An orthophoto of HiRISE image PSP_003816_1245. White lines mark the locations of profiles in Figures 7g–7i derived from the DEM. (g) An example of a cross-sectional profile showing that individual layers occur within ~1 m of the same elevation on both sides of the ridge. Three prominent layers have been marked (1a–1b, 2a–2b, and 3a–3b). (h) An example of a profile tracing a layer along the length of the ridge. Layers, such as the one seen here, exhibit slight undulations and slope gently downward to the north, but are essentially horizontal. The slope seen here is ~0.87°. (i) Examples of two MOLA PEDR tracks (red) compared with profiles acquired from the HiRISE DEM (blue). Elevations from the two data sets differ by a maximum of ~10 m and usually differ by only a few meters.

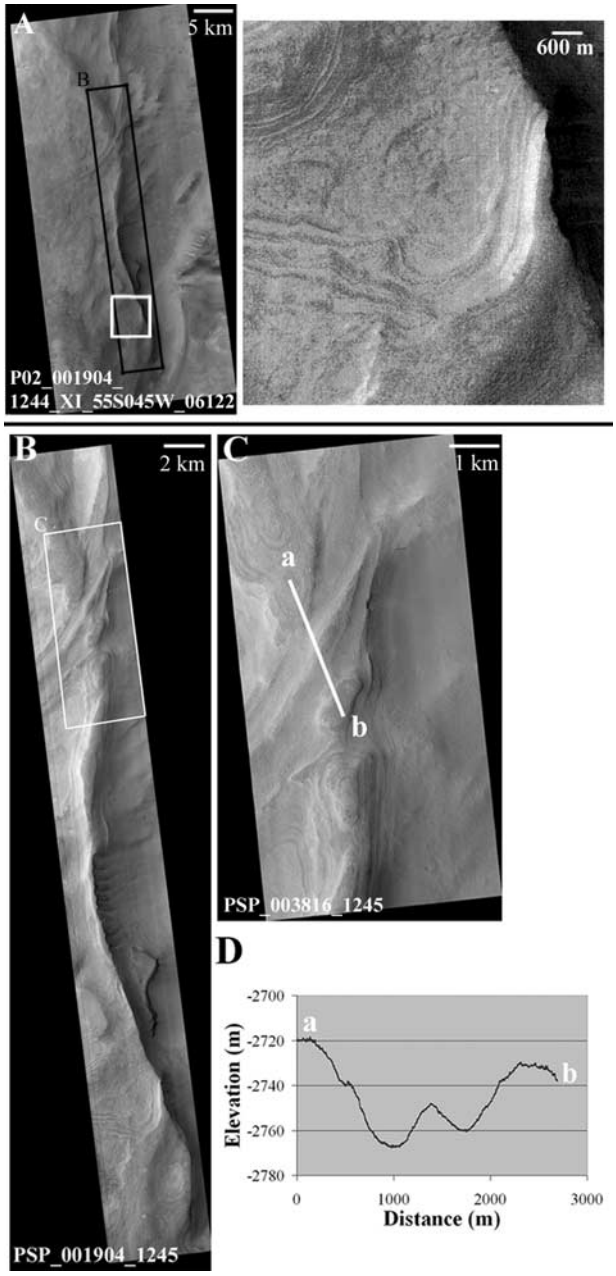

Figure 8. A portion of Cleia Dorsum where it lies at the edge of a depression (to the east). (a) In a CTX image of Cleia Dorsum (P02_001904_1244_XI_55S045W_06122), layers appear to extend into the surrounding topography on the west side of the ridge. The white box (left) outlines the location of the enlargement (right). The black box outlines the location of the image in Figure 8b. (b) HiRISE image PSP_001904_1245. The white outline marks the location and area covered by a DEM created using HiRISE stereo pair PSP_003816_1245 and PSP_004106_1245 (see Figure 7) and the orthophoto in Figure 8c. This portion of Cleia Dorsum is crosscut by a secondary ridge that extends to the northeast. (c) Orthophoto of PSP_003816_1245. The white line marks the location of the profile in Figure 8d. (d) A profile, derived from the HiRISE DEM, across a secondary ridge that crosscuts Cleia Dorsum. Large grooves carved into the secondary ridge are U shaped.

close to the shore and parallel the coastline. While spits are barriers that are connected to the shore at one end, barrier bars are not connected to the shore at either end. Terrestrial barrier bars, in particular, have dimensions similar to the Argyre ridges and can extend for long distances (typically up to 100 km) and have widths up to several kilometers [*Easterbrook*, 1999]. *Parker* [1994] notes that ridges radial to Surius Vallis appear primarily east of the channel mouth, and form counterclockwise arcs across the basin floor roughly paralleling the southern edge of the basin. If the basin was filled with water at the time of ridge formation, the distribution of the ridges suggests that there was a dominant paleowind direction toward the southeast and sufficient wave energy to deflect channel outwash sediments, entering the basin through Surius Vallis, eastward along the basin margin [*Parker*, 1994]. However, this hypothesis does not explain the formation of ridges that trend north and northwest, such as Cleia Dorsum and the ridges north and west of Oceanidum Mons (Figure 2). The hypothesis also does not explain the occurrence of the northeast trending ridge that crosscuts the northwest trending Cleia Dorsum (Figure 8). Terrestrial spits and bars associated with a single river mouth are typically much shorter than the Argyre ridges as well, although this scale difference may be partly due to lower Martian gravity [*Parker et al.*, 1986]. In addition, terrestrial spits and bars do not typically occur as sets of multiple ridges (especially with differing orientations) and typically do not form branching and braided patterns like those observed in the Argyre ridges. Whereas lacustrine spits and bars are a possible analog for Argyre from the perspective of expected wave and current energy, marine barrier islands constitute another possible analog at an extreme high energy range. Exemplified by the Outer Banks of North Carolina, barrier islands are characteristically arcuate in plan view, and individual cuspate barrier islands link together to form cuspate or scalloped chains of islands, with cuspate segments oriented so that they are convex toward the shore. Whereas the spatial scales are comparable, this is not the observed geometry of the sinuous ridges in Argyre which are indeed sinuous, not cuspate or scalloped. Other types of coastal ridges include coastal dunes and ridges formed by sea ice interactions with the shore [*Forbes and Taylor*, 1994].

[16] The Argyre sinuous ridges are also similar to glacial moraine deposits such as terminal or end moraines. End moraines form at the ice margin as symmetric and asymmetric ridges that may be sinuous, arcuate, or lobate in plan view, and can merge and bifurcate [*Benn and Evans*, 1998]. While the height and width of some terrestrial end moraines is similar to the Argyre ridges [*Benn and Evans*, 1998; *Hiesinger and Head*, 2002], terrestrial moraines are typically much shorter in length and are frequently broken by gaps giving them a much lower continuity [*Benn and Evans*, 1998]. Moraines are also typically composed of unstratified glacial sediments and thus most do not have layers [*Benn and Evans*, 1998]. A related possibility is that the Argyre sinuous ridges could represent crevasse fillings, or debris that accumulated in the crevasses of stagnant ice and lowered to the surface by ablation [*Kargel*, 1993; *Martini et al.*, 2001]. However, terrestrial crevasse fill ridges are typically much lower in height (up to 10 m) than the Argyre ridges, and are relatively short in length (a few tens of meters long) [*Martini et al.*, 2001].

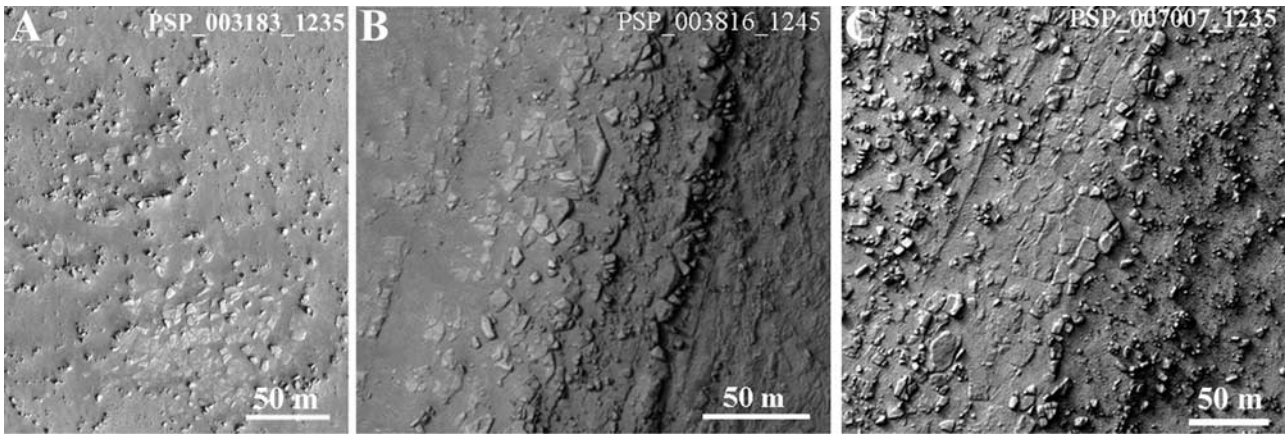

Figure 9. Large boulders, some greater than 8 m in scale, are observed in layers and on ridge surfaces. The boulders tend to be angular in shape and are generally not observed in the same abundance on the surrounding terrain. (a) Close-up view of the surface of Pasithea Dorsum (HiRISE image PSP_003183_1235). (b) Close-up view of layers in Cleia Dorsum (HiRISE image PSP_003816_1245). (c) Close-up view of layers in Pasithea Dorsum (HiRISE image PSP_007007_1235). Many of the large boulders, particularly angular ones, appear to be interlocking and eroding out of indurated or cemented layers. Most likely, these are not discrete boulders that were transported but rather are a lag forming from fracturing and erosion of indurated layers of smaller, relatively fine-grained material that was transported and deposited in the ridges. Whether some of the large boulders may have been transported, perhaps those that are more rounded, is unclear.

[17] Altogether, the characteristics of the Argyre sinuous ridges are most consistent with landforms that have a fluvial origin, such as inverted streams or eskers. For example, using comparisons of sinuosity, *Kargel* [1993] found the Argyre ridges best resembled terrestrial river channels and eskers as opposed to terrestrial linear sand dunes or wrinkle ridges. Inverted stream topography on Earth forms when a former valley floor is protected or becomes more resistant to erosion than the surrounding surface. Over time, erosion of the less resistant adjacent material exposes the former valley floor as a sinuous ridge. Wind action appears to be the most common erosive process on Mars capable of producing relief inversion [*Pain et al.*, 2007]. If the Argyre ridges represent inverted stream topography, a significant amount of wind erosion is necessary to expose these landforms as they are today (at least 300 m of vertical erosion). Although not conclusive, the Argyre ridges exhibit several characteristics that would not be expected in typical inverted channels such as very low and high tributary junction angles [*Pain et al.*, 2007], branching V's that open in opposing directions rather than a single upstream direction [*Ruff and Greeley*, 1990], and longitudinal discontinuities [*Pain et al.*, 2007].

[18] The topographic analysis indicates that the elevation at which the ridges occur varies along trend for all three of the ridges analyzed. In open river channels, water flow is driven by gravity to follow topographic gradients and flow downhill. Assuming that the regional topographic gradient has not changed since the formation of the ridges, the fact that the ridges cross topography indicates that they were formed by pressure-driven flow rather than gravity-driven flow, which is not consistent with open terrestrial river channels. On the other hand, terrestrial eskers commonly climb and cross topographic divides. Eskers are ridges composed of stratified glacial drift deposited by a supraglacial, englacial, or subglacial stream of flowing water (Figure 14). As the ice retreats, deposited sediments are exposed as a long, winding ridge (esker) on what was previously the subglacial floor [e.g., *Benn and Evans*,

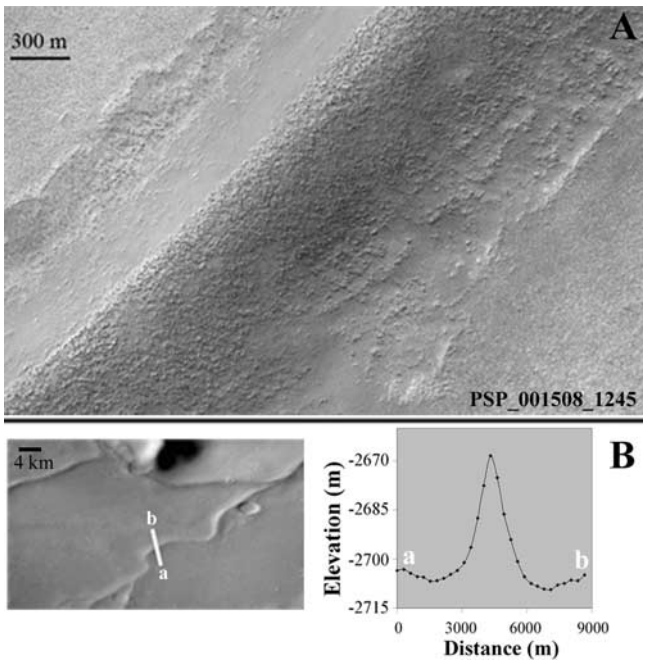

Figure 10. Portions of Argyre sinuous ridges are observed within shallow troughs. (a) HiRISE image PSP_001508_1245 shows a section of Pasithea Dorsum lying within a trough. (b) A profile derived from MOLA PEDR data showing another portion of Pasithea Dorsum where it occurs within a trough. (left) The location of the profile is indicated with a white line in the THEMIS daytime IR mosaic (http://jmars.asu.edu).

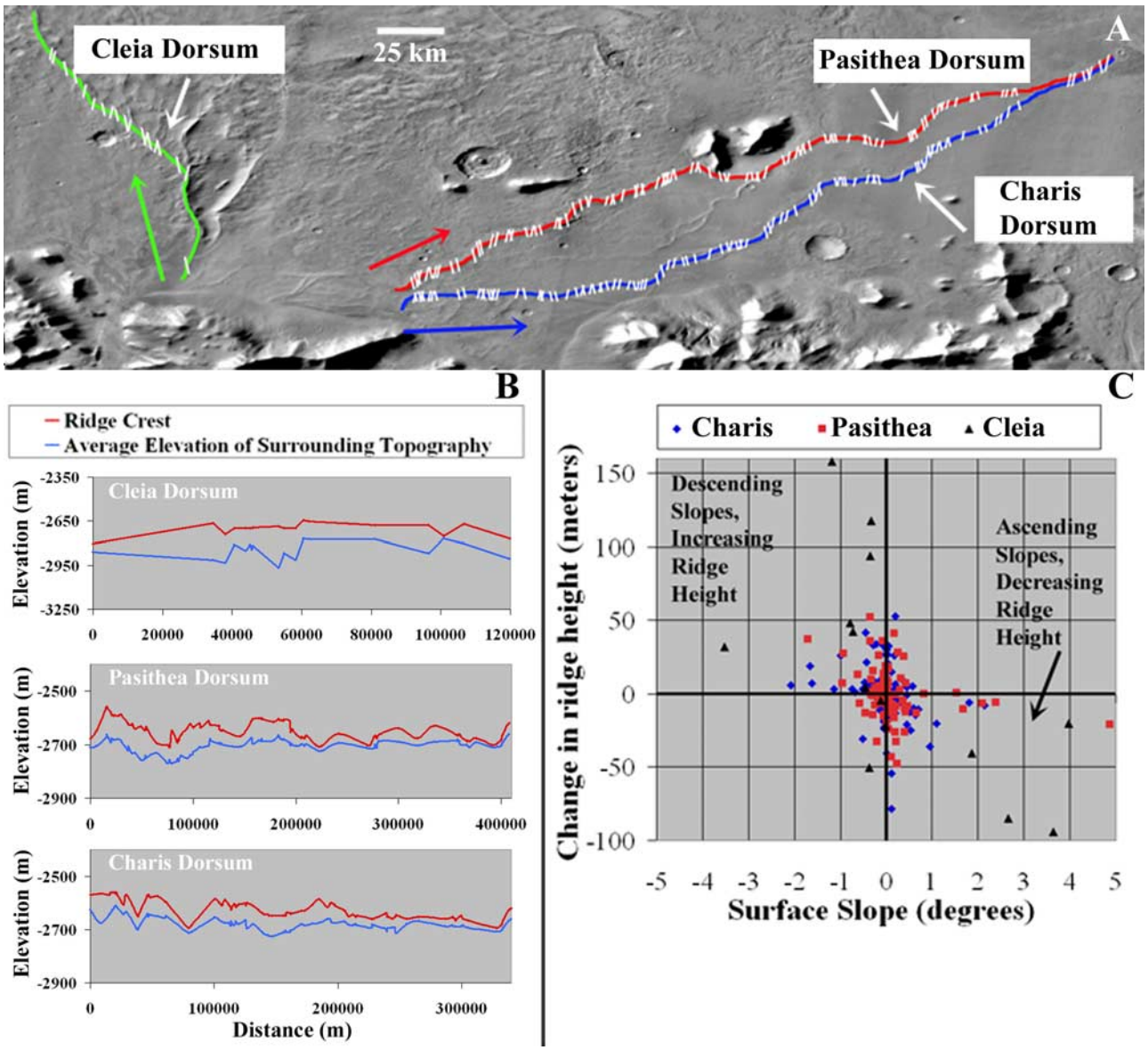

Figure 11. Topographic analysis of the Argyre sinuous ridges. (a) The locations of the three ridges used in the topographic analysis are marked in green (Cleia Dorsum), red (Pasithea Dorsum), and blue (Charis Dorsum) on a THEMIS daytime IR mosaic (http://jmars.asu.edu). Multiple cross-sectional profiles were derived from MOLA PEDR tracks along the extent of the three ridges. White lines in the mosaic indicate the locations of the MOLA tracks used in this analysis on each of the ridges. The direction along each ridge in which the data were plotted in Figure 11b is indicated by colored arrows next to the three ridges. (b) The elevation of the surrounding surface was averaged at each profile location in Figure 11a and plotted as a function of distance along the extent of each ridge (blue lines). For each of the ridges, the overall elevation at which they occur varies along trend, indicating that the Argyre ridges cross topography. The height of each ridge was also plotted (red lines) and found to vary along the extent of each ridge. The vertical exaggeration differs for each plot. (c) The change in ridge height between successive MOLA tracks along each ridge was plotted against the average slope of the surrounding surface. For slopes greater than 1°, ridge height increases with descending slopes and decreases with ascending slopes. This is a characteristic observed in terrestrial eskers that is related to flow processes.

1998; *Easterbrook*, 1999; *Brennand*, 2000]. Eskers deposited by meltwater flowing in an englacial or subglacial ice tunnel or subice streambed, can cross topography because the water is under hydraulic pressure. Flow in eskers is dictated by glacier surface topography and internal structure with only a small component contributed by the gradient of the bed. Ice thickness, or the weight of overlying ice, influences water pressure at the base of the ice and enables subice streams to cross topography [e.g., *Röthlisberger*, 1972; *Shreve*, 1985]. *Hiesinger and Head* [2002] and *Lang* [2007] also found

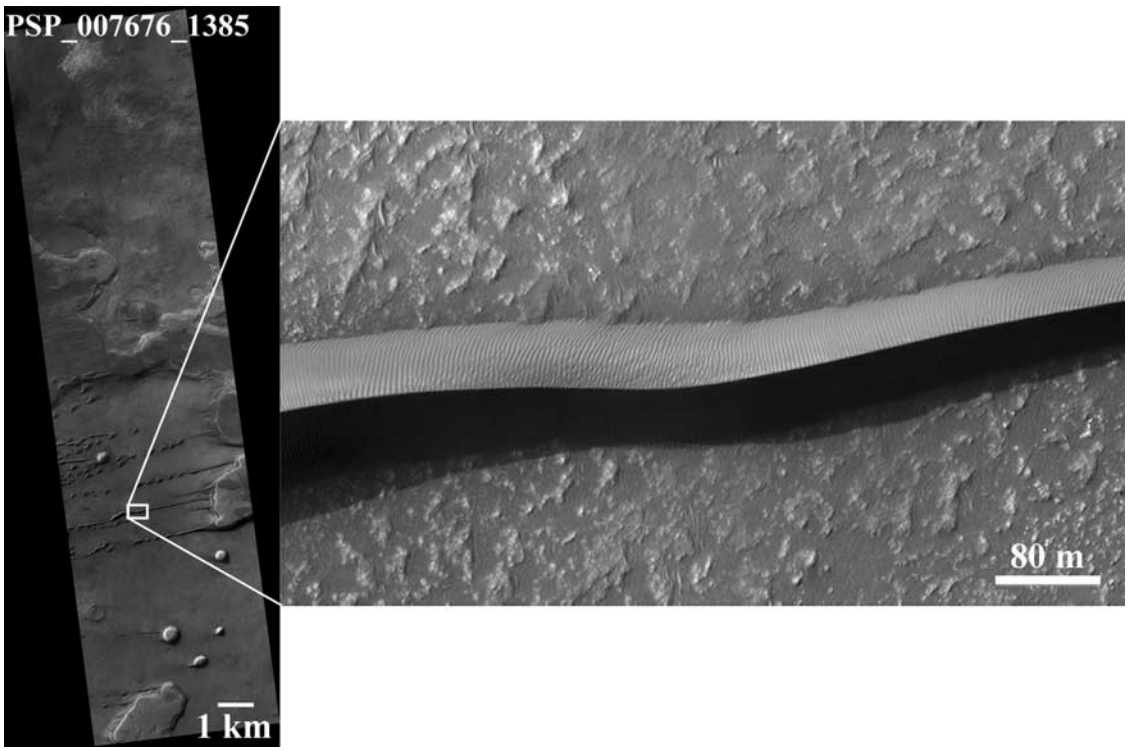

Figure 12. (left) Linear sand dunes and barchan dunes in a crater in the Hellespontus region of Mars (HiRISE image PSP_007676_1385). Net wind direction is approximately east to west. Typical terrestrial linear dunes, as well as typical Martian dunes, are shorter, thinner, and lower in height than the Argyre ridges and more closely spaced. (right) The linear dune seen in the enlargement, like most Martian dunes, has ripples superposed on its surface, does not show layering, and is not lying within troughs.

that the Argyre ridges cross topography leading them to favor the esker interpretation, as did topographic analyses of similar sinuous ridges in the Dorsa Argentea Formation [e.g., *Head*, 2000a, 2000b; *Head and Hallet*, 2001a, 2001b; *Head and Pratt*, 2001; *Ghatan and Head*, 2004].

[19] The relationship of ridge height and crest shape to the slope of the surrounding surface is also consistent with observations of terrestrial eskers. In descending ice tunnels, viscous heat produced by flow of meltwater causes melting of the tunnel walls increasing the height of the tunnel and the resulting esker ridge. Meltwater flowing in ascending tunnels has less viscous heat resulting in freezing of water onto the walls of the tunnel and, consequently, the formation of shorter ridge heights [*Shreve*, 1985]. In a similar way, the surface slope also influences the shape of the esker. Strong melting in descending or level tunnels forms sharp-crested eskers while weaker melting can form a multiple-crested esker. In ascending tunnels, water usually freezes to the top of the tunnel first forming a lower, broader, and more rounded esker shape [*Shreve*, 1985]. This relationship between ridge height and shape and the surrounding surface slope was observed by *Shreve* [1985] in the Katahdin esker system of Maine. A similar relationship between the shape of the sinuous ridges in the Dorsa Argentea Formation and the slope of the surrounding topography was observed by *Head and Hallet* [2001a, 2001b]. *Hiesinger and Head* [2002] also noted that the majority of the profiles for one of the main Argyre ridges revealed a single relatively sharp crested ridge shape, which is consistent with the primarily flat surrounding surface in the southern Argyre basin.

[20] Our interpretation of the topographic analysis assumes that the regional topographic gradient has remained stable since formation of the ridges. Our interpretation also assumes that differential erosion since ridge formation has not created all of the undulations observed in the surrounding surface or significantly altered ridge crest shape and height along the extent of the ridges. The lack of tectonic structures in the Argyre Planitia suggests that this region has not been subjected to tectonic processes relatively recently [*Zuber et al.*, 2000; *Hiesinger and Head*, 2002]. Changes in ridge height and shape also appear to be consistently related to the slope of the surrounding topography; this would not necessarily be the case if changes to the slope of the surrounding topography had taken place subsequent to ridge formation, or if the ridge shape and height had been significantly altered by differential erosion. This characteristic is also difficult to explain within the context of the other formation hypotheses.

[21] The results of the topographic analysis, along with several other characteristics of the ridges mentioned above, indicate that the sinuous ridges resemble terrestrial eskers more closely than terrestrial examples of inverted stream topography. Like the Argyre ridges, terrestrial eskers are extremely variable and can range in form from single, continuous ridges to complex braided and dendritic systems with confluent and diffluent branches [e.g., *Benn and Evans*, 1998], and have undulating crests which vary in shape owing to flow processes [*Shreve*, 1985; *Benn and Evans*, 1998]. The

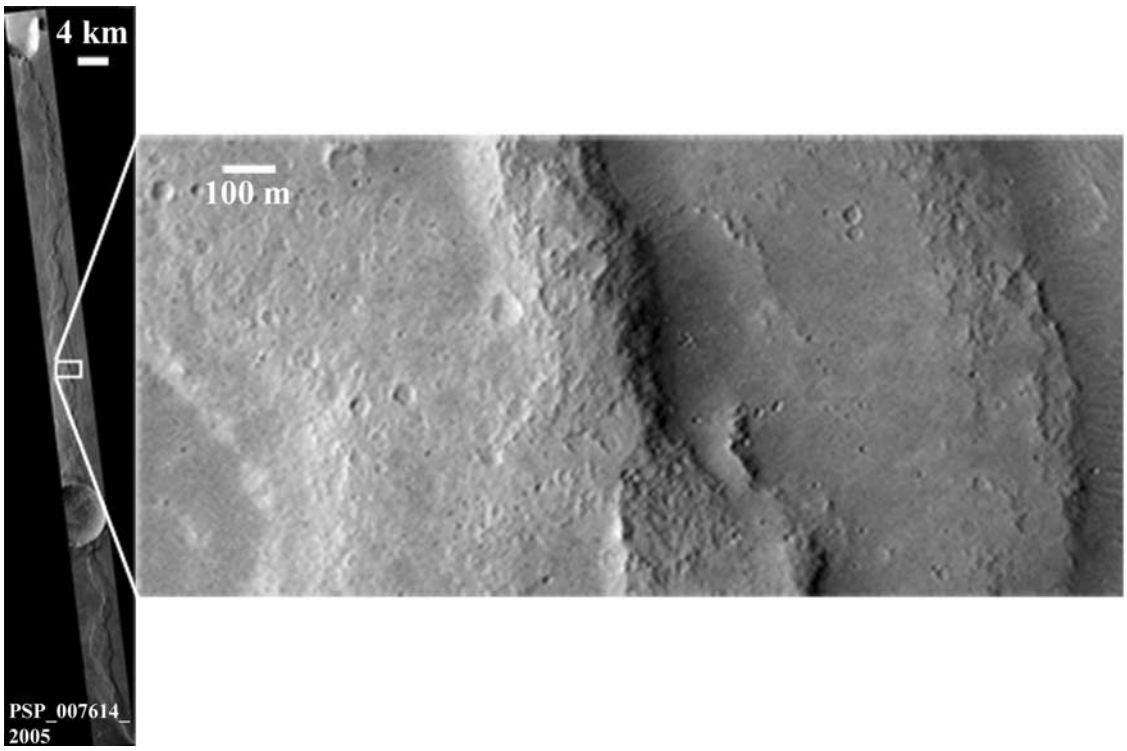

Figure 13. (left) A wrinkle ridge in Lunae Planum, Mars (HiRISE image PSP_007614_2005). Wrinkle ridges tend to be slightly lower in sinuosity compared to the Argyre ridges. (right) This enlarged wrinkle ridge exhibits a smaller, steep hill on top of a broad arch. This morphology is common for Martian wrinkle ridges but is not commonly observed in the Argyre ridges. HiRISE images of wrinkle ridges also reveal that these features vary from the Argyre ridges in their detailed structure and surface texture, do not contain horizontal layers, and are not typically observed in troughs.

Argyre ridges are also similar to terrestrial eskers in their sinuosity, branching patterns, and very low and high tributary junction angles which, in terrestrial examples, can occur owing to control of streamflow by crevasses, pressure ridges, and when present, medial moraines, and other glacial structures [*Kargel and Strom*, 1992; *Kargel*, 1993]. Although the troughs surrounding portions of the Argyre ridges may be the result of erosion subsequent to formation of the ridges, the appearance of the ridges in troughs is also consistent with the esker hypothesis; terrestrial eskers sometimes occur within larger valleys or troughs, often referred to as Nye channels (N channels) or tunnel valleys, that form from abrasive subglacial meltwater discharge that erodes into bedrock or sediments [*Benn and Evans*, 1998; *Shreve*, 1985].

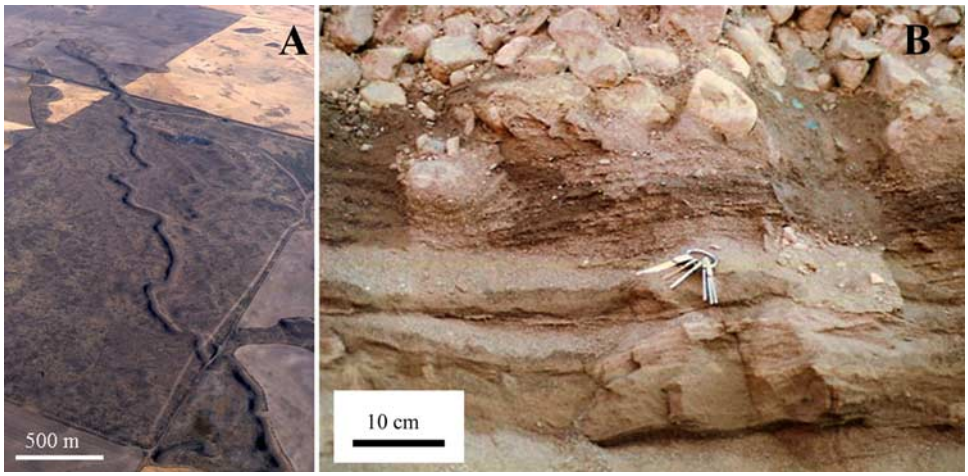

Figure 14. Terrestrial eskers. (a) Aerial view of an esker on the Waterville Plateau, eastern Washington (photo by V. Baker). (b) Variations in layering in a small esker within the much larger Devil's Track esker complex near Grand Marais, Minnesota (photo by J. Kargel).

[22] Terrestrial eskers may contain horizontal or near horizontal beds or layers (Figure 14b) [e.g., *Benn and Evans*, 1998; *Huddart et al.*, 1999]. These layers can be continuous for considerable distances or taper out quickly [*Easterbrook*, 1999], and can form alternating or cyclic sequences as do layers observed in the Argyre sinuous ridges [*Benn and Evans*, 1998]. Variations in the layers of terrestrial eskers are often attributed to fluctuations in discharge due to seasonal and/or annual changes [*Bannerjee and McDonald*, 1975; *Brennand*, 1994; *Benn and Evans*, 1998]. Likewise, alternating patterns of layers observed in portions of the Argyre ridges (Figure 6) may be the result of fluctuations in meltwater discharge and availability and/or sediment availability on Mars.

[23] The esker hypothesis is favored by the location of the Argyre ridges in the Martian middle latitudes (>50°S). Several studies have interpreted landforms in the Martian midlatitudes to be the result of large accumulations of ice [e.g., *Kargel and Strom*, 1992; *Kargel et al.*, 1995; *Mangold*, 2003; *Kargel*, 2004; *Head et al.*, 2005]. Recent results from the Shallow Radar (SHARAD) instrument onboard MRO, have detected large accumulations of water ice in lobate debris aprons in the eastern Hellas region (~33.7–47.4°S, 90.8–114.3°E), supporting the hypothesis that the lobate debris aprons are debris covered glaciers [*Holt et al.*, 2008]. The SHARAD results imply that previous climatic conditions on Mars were conducive to the accumulation of large ice masses in the middle latitudes. Sets of sinuous ridges are observed in different locations on Mars and may plausibly have varying formation mechanisms; on Earth there are plentiful examples of both sinuous ridges that represent inverted fluvial streams and ridges that are eskers. Most sinuous ridges on Mars interpreted as inverted streams occur between 40°N and 50°S [*Pain et al.*, 2007].

[24] The esker hypothesis is further supported by evidence of past glaciation identified in the surrounding Argyre region. Landforms in the Argyre Planitia and adjacent Charitum Montes have been interpreted as a glacial suite of cirques, horns, U-shaped valleys, drumlins, kettles, and outwash plains formed by glacial erosion and deposition [e.g., *Kargel and Strom*, 1992; *Baker*, 2001; *Hiesinger and Head*, 2002; *Kargel*, 2004; *Banks et al.*, 2008; *Banks*, 2009]. HiRISE imagery has recently revealed additional landforms in the surrounding Charitum and Nereidum Montes that are potentially glacial in origin including long linear grooves, streamlined hills consistent with glacially sculpted bedrock, and large, unsorted, boulder-rich deposits interpreted as morainal material [*Banks et al.*, 2007, 2008; *Banks*, 2009].

[25] Some characteristics of the ridges however, remain partially inconsistent with those of typical terrestrial eskers. For example, the Argyre ridges differ from most terrestrial eskers in continuity and total length. Terrestrial eskers have an average continuity of roughly 60% while the Martian sinuous ridges have a continuity closer to 97%. [*Metzger*, 1992]. Gaps in terrestrial eskers are partly due to postglacial erosion [e.g., *Metzger*, 1992] and the higher continuity of the ridges on Mars could be a partial result of lower erosion rates. Discontinuous terrestrial eskers also often indicate englacial or supraglacial flow in which the esker form is disrupted as the esker settles to the valley floor during retreat of the ice [*Brennand*, 2000]. The continuous nature of the Argyre ridges could indicate that they formed primarily by flow at the base of the ice rather than englacial or supraglacial flow [*Metzger*, 1992]. This is also supported by the preservation and lack of deformation in the layers observed in HiRISE images (Figure 6). However, it should be noted that within an individual terrestrial esker or esker system, water can flow via supraglacial channels, englacial/subglacial conduits, and ice-walled canyons near ice margins, and thus some combination of these is possible [e.g., *Benn and Evans*, 1998; *Huddart et al.*, 1999].

[26] Another concern regarding the esker hypothesis is the large dimensions of the Argyre ridges and their aspect ratio. Although typical terrestrial eskers are smaller, the dimensions of the Argyre ridges correspond to the upper limit of terrestrial eskers: up to roughly 300 m high, 3 km wide, and 500 km long (with breaks) [*Ritter et al.*, 2002; *Hooke*, 2005]. For example, *Mangold* [2000] found the dimensions of giant paleoeskers in Mauritania to be on the same order of magnitude as those of the Argyre sinuous ridges. Typical terrestrial eskers also differ from the Argyre ridges in their aspect ratio; terrestrial eskers tend to be taller relative to their widths and have steeper side slopes than the Argyre ridges. However, the aspect ratio of the Argyre ridges is consistent with what is expected for a very large discharge; as discharge increases in terrestrial streams, the streams preferentially become wider as opposed to deeper, or in the case of eskers, wider as opposed to taller. In addition, the aspect ratio of the Argyre ridges is consistent with that of the large eskers in Mauritania whose heights measure up to 150 m with widths of ~1.5 km [*Mangold*, 2000].

[27] In a terrestrial ice marginal environment, one might also expect to find outwash fans and terminal or end moraines [*Brennand*, 2000]. These features have not been conclusively observed in the area of the Argyre sinuous ridges. The lack of end moraines, however, may be due to the way in which the ice retreated. Two common types of ice terminus retreat are active retreat and stagnant retreat. In active retreat, continuous forward flow of the glacier builds moraine ridges, such as end moraines, but typically degrades or distorts and even destroys esker deposits. In stagnant retreat, stagnation of the ice minimizes the formation of end moraines and enhances preservation of an esker system [*Metzger*, 1992; *Benn and Evans*, 1998; *Head*, 2000a]. If the ridges in the southern Argyre basin represent an esker system, their preservation as long, continuous sections with well defined and continuous layers indicates that they formed during extensive stagnant retreat of an ice terminus and thus, large end moraines may simply not have formed. Possible outwash fans may be heavily mantled and remain undetected in currently available imagery or perhaps, like end moraines, did not form. *Metzger* [1992] found that eskers in New York state rarely terminated in deltaic fans and were rarely seen in close association with terminal moraines.

4. Environmental Implications

[28] The map patterns and morphology of the Argyre ridges, their occurrence in troughs, ability to cross topographic divides, the relationship of their height and crest shape to the slope of the surrounding surface, location at >50°S latitude, and the occurrence of other potential glacial landforms in the surrounding region, support the esker

Table 1. Summary of Analysis[a]

Hypothesis	Planform Patterns and Sinuosity	Morphology and Dimensions	Horizontal Bedding	Location Within a Trough	Cross Topography, Increasing Ridge Height on Descending Slopes, and Decreasing Height on Ascending Slopes
Sand dunes	No	Yes	No	No	Yes
Wrinkle ridges (tectonic ridges)	No	Maybe	No	No	Yes
Lava flow features	No	Maybe	Yes	Maybe	Maybe
Igneous dikes	Maybe	Yes	No	Maybe	Yes
Lacustrine spits and barrier bars	No	Yes	Yes	Maybe	No
Glacial moraines and crevasse fill ridges	Maybe	No	Maybe	Maybe	Yes
Inverted fluvial channels	Yes	Yes	Yes	Yes	No
Eskers	Yes	Yes	Yes	Yes	Yes

[a]The first column lists the different formation hypotheses, and the top row of the table lists the characteristics of the Argyre sinuous ridges discussed in this study. A "yes," "no," or "maybe" is used to indicate which formation mechanisms are consistent with the observed ridge characteristics. The only formation mechanism consistent with all of the observed ridge characteristics is the esker hypothesis.

hypothesis and indicate that the ridges are most likely eskers formed by glaciofluvial processes. Table 1 summarizes our analysis. Using terrestrial eskers as an analog, several aspects of the environment in which the Argyre sinuous ridges formed can be inferred.

[29] On Earth, eskers form at the margins of large deposits of retreating or stagnating ice. Thus, the presence of ridges interpreted as eskers suggests that the southern Argyre Planitia was once covered by a large ice deposit. From the distribution of the Argyre ridges, it can be inferred that this ice extended for hundreds of kilometers or more within the basin and reached northward to a latitude of at least ~52°S. The height of the ridges indicates that the ice covering was once more than 300 m thick and probably much thicker. *Hiesinger and Head* [2002] estimated the ice thickness to be on the order of ~2000 m. During the period of ridge formation, the ice was stagnating or retreating, its margin was located in the southern portion of the Argyre basin near the area of ridge exposure, and water was flowing within or beneath the ice. This ice may have been part of an ice sheet [*Kargel*, 1993, 2004], a glacier or multiple glaciers that entered the basin from the south [*Kargel and Strom*, 1992], or a frozen lake in the basin [*Hiesinger and Head*, 2002]. *Hiesinger and Head* [2002] proposed a model in which meltwater from a Hesperian meltback of the south polar ice sheet entered the basin through channels to the south and southeast and partly filled the basin to form a lake. In their model, the lake froze to the ground, at least in the shallow marginal regions, and meltwater from the frozen lake and/or incoming water from the south, formed channels at the base of the ice in which the ridges were deposited. Several of the ridges appear to radiate from the mouth of Surius Vallis, a valley that opens into the Argyre basin from the south (Figure 2), suggesting that water may have entered the frozen Argyre basin through this channel and flowed beneath the ice in primarily north and northeastly directions.

[30] In comparison to average Earth esker analogs, the Argyre sinuous ridges are larger in width, height, and extent. Assuming similar processes were involved in esker formation under Martian conditions, this may indicate that sediments and meltwater were available in larger quantities and/or available for longer periods of time on Mars than during typical esker formation on Earth. *Metzger* [1991, 1992] estimated the duration of glaciation required to form eskers of this size as longer than that of the late Wisconsin deglaciation. Evidence of substantial glacial erosion in the surrounding Charitum and Nereidum Montes (lower limit for the volume of eroded material on the order of $\sim 4 \times 10^3$ km^3) [*Banks*, 2009] has also led to estimates of a period or periods of glaciation that lasted for potentially several million years or longer [*Kargel*, 2004; *Banks et al.*, 2008; *Banks*, 2009].

[31] Assuming the sinuous ridges were formed by subice fluvial processes, HiRISE imagery and MOLA data can be used to make predictions of the velocity and discharge involved in their formation. Available constraints are insufficient to define the problem uniquely, especially since so much depends on processes and key parameters, not all of which are definitively resolved or defined. For example, to what degree were channel full conditions involved, and what was the hydraulic head going into the channel and that at the nozzle? Could flow have been river-channel-like at times, either in a tunnel that was not filled completely or which was, in places, open to the sky? What was the geometry of the channel? Observations indicate that pressurized channel-full conditions were most likely involved (e.g., to drive flow up undulations of the bed, as documented above), and so we focus on this condition, without rejecting a situation more akin to terrestrial river flow or unfilled channel flow conditions. Of course, if the ridges are eskers formed in subice tunnels, pressurized channel-full conditions were involved at least for some period of time.

[32] Here we calculate the approximate velocity and discharge using a reduced form of the Darcy-Weisbach equation, where head loss and pipe length are removed as terms [*Lorang and Hauer*, 2003]. This equation is appropriate for estimating the velocity of past potential water flows on Mars and is used here to estimate flow in a subice conduit under marginally pressurized (i.e., water fills the subice channel) conditions [*Komar*, 1979; *Lorang and Hauer*, 2003]:

$$u = \sqrt{\frac{8}{f_r} gRS_f} \tag{1}$$

where u is the mean velocity, f_r is the dimensionless Darcy-Weisbach friction coefficient, g is the acceleration due to gravity, R is the hydraulic radius, and S_f is the friction slope with the channel bottom slope, S, being used as a first-order

approximation to S_f [*Lorang and Hauer*, 2003]. S is used here as a rough lower-limit approximation of the hydraulic gradient of the ice using an assumption that the ice surface slope roughly mimics the bed topography. The hydraulic radius, R, is the cross-sectional area, A, divided by the wetted perimeter, P ($R = A/P$). In this study, the cross-sectional shape of the channel is simplified as a low, broad triangle. A representative width of 2 km was chosen on the basis of the ridge dimensions. Flow depths (h) of 1 m and 10 m were chosen on the basis of comparison to terrestrial proglacial streams; water depths in terrestrial proglacial streams are typically up to several meters over a bed of coarse sand and gravel (grain sizes commonly observed in terrestrial eskers) [*Benn and Evans*, 1998]. The lower value of h, 1 m, would appear less than the likely depth given the great width of the system, whereas the upper value, 10 m, would not likely be exceeded according to typical terrestrial examples; hence, we probably bracket the actual value, but there is no certainty of this. The values of width and flow depth were used to determine A (1×10^3 m^2 ($h = 1$ m); 1×10^4 m^2 ($h = 10$ m)), and P (4×10^3 m). For channel full flow, values of 0.25 and 2.5 m were calculated as approximate lower and upper estimates for R. An overall change in elevation of ~300 m over the extent of the Argyre ridges, ~300 km, was determined using MOLA interpolated data and used to estimate a slope of 0.001. Using 3.72 m/s^2 for g, f_r was determined using the relationship [*Leopold et al.*, 1964]

$$\frac{1}{f_r^{0.5}} = 2\log(h/D_{84}) + 1.0 \tag{2}$$

where h is the flow depth (1 m and 10 m), and D_{84} is the grain diameter of the channel bed sediments of which 84% of the total grain size distribution is finer. As terrestrial eskers are commonly composed of gravel and sand sized particles [*Benn and Evans*, 1998], minimum and maximum values of 0.5 mm and 64 mm are used for D_{84} to represent medium sand to very coarse gravel grain sizes, respectively [*Wentworth*, 1922]. Equation (2) is comparable to equations for friction factors for pipe flow with a large range of relative roughnesses. Also, the f coefficient of this relationship, unlike the Chezy and Manning n coefficients, does not have to be corrected for the gravity field and thus can be employed to evaluate drag coefficients for water flows on Mars as well as Earth [*Komar*, 1979]. Using h = 1 m and 10 m, and D_{84} = 0.5 mm and 64 mm, values ranging from 0.01 to 0.087 were calculated for f_r. Mean velocities ranging from 0.29 m/s to 2.6 m/s were then calculated using equation (1) with an average of ~1.3 m/s. The above calculations assume fluid flow as opposed to matrix supported debris flow. An average velocity of ~1.3 m/s is slightly lower than the velocity of the Mississippi River (2 to 3 m/s) [*Komar*, 1979], and is comparable to paleovelocities calculated for the Bridgenorth esker (0.05 to 3.5 m/s) located in Ontario, Canada [*Jackson*, 1995]. Because of the lower gravity, the same bottom stress values on Mars can move larger grain diameter material than on Earth and flows of this velocity on Mars would most likely be very erosive and able to transport considerable amounts of material [*Miller and Komar*, 1977; *Komar*, 1979].

[33] The discharge (Q) of flow along the ridges is given by [e.g., *Komar*, 1979]

$$Q = uA \tag{3}$$

and is on the order of ~1×10^4 m^3/s. It should be noted that a highly pressurized flow would have a steeper velocity gradient and thus an increased velocity of flow and discharge; therefore a discharge of ~1×10^4 m^3/s should be considered a lower limit. Considering the number and length of the ridges (hundreds of kilometers), and assuming that they formed contemporaneously, the discharge was most likely substantial [*Metzger*, 2002] and large quantities of ice and subsequent meltwater would have been necessary to deliver sufficient water to the subice drainage network to form the ridges. When considering the characteristics of the ridges as a whole, the large dimensions (up to hundreds of meters tall and several kilometers wide), aspect ratio, extent (hundreds of kilometers), and other characteristics of the eskers, are all also consistent with a large discharge. This adds support to the *Hiesinger and Head* [2002] model in which meltwater flows into the Argyre area from the south, through valleys such as Surius Vallis, as opposed to originating as meltwater derived from melting of ice in the Argyre area only.

[34] Several assumptions and approximations were used in the above calculations regarding factors such as channel bed grain size (D_{84}) and overall frictional forces, average surface slope/hydraulic gradient of the ice, and the average cross-sectional area of the subice channel. In particular, the hydraulic gradient of the ice was most likely greater than the gradient of the bed topography and thus the velocity of the flow was most likely higher under pressurized conditions. Noting that possible water sources of the ridge-forming flows occur outside Argyre in the highlands, the total topographic drop is several kilometers. Depending on where the water enters an englacial or subglacial tube, the potential exists for very large hydraulic pressurization. Therefore, the above calculations should be viewed as approximate lower limits only. Clearly there is a potential for flow conditions comparable to those of large terrestrial rivers, which presumably would have to operate over very long periods of time (centuries at least, maybe many millennia) to deposit ~100 m thick bed sequences. Or it is possible that more rapid flow processes occurred under high hydraulic pressure, which could have driven flow of highly erosive and sediment-rich channel fluid and could have deposited the bed sequences rapidly once pressure was relaxed. The available constraints, unfortunately, do not permit us to better constrain the solution at this time.

[35] The preservation of long, continuous ridges and the lack of obvious moraine deposits indicates that extensive stagnant retreat of the ice terminus is more likely than active retreat. The continuous nature of the ridges and the preservation of distinct layers also suggests that the ridges primarily formed in tunnels at the base of the ice; eskers deposited in englacial or supraglacial streams are much more likely to become disrupted and broken from settling to the ground as the ice retreats [*Brennand*, 2000]. The appearance of eskers in troughs may indicate synchronous patterns of deposition and erosion at the glacier bed or, more likely, a period of erosion followed by deposition and tunnel infilling; possibly a result of falling discharges [*Benn and Evans*, 1998]. Either

way, eskers lying within eroded channels provide further evidence that the conduit was subglacial rather than englacial or supraglacial, at least in places, and was a relatively stable part of the glacier bed [*Benn and Evans*, 1998].

[36] The secondary northeast trending ridge that crosscuts Cleia Dorsum (Figures 2 and 8) may have formed owing to a shift in the flow of water within or beneath the ice or perhaps a subsequent phase of glaciation. Shifts in the direction of esker flow in terrestrial glaciers can occur owing to changes in the flow of the ice or changes in the surface of the ice which alter the hydraulic gradient. The U shape of the large grooves carved into the secondary ridge is a typical morphology for landforms eroded by flowing ice masses, and offers further support for the past presence of ice at this location. The occurrence of U-shaped grooves in the crosscutting ridge indicates a period of erosion subsequent to the shift in water flow direction.

[37] Layers in terrestrial eskers, similar to those observed in portions of the Argyre ridges, can arise from subtle changes in the basal hydrology of the ice and may indicate fluctuations in meltwater discharge and availability, and/or sediment availability [*Benn and Evans*, 1998]. Patterns of alternating layers suggest that the layers formed in a cyclic manner; this could be related to seasonal, annual, or potentially even obliquity changes [*Bannerjee and McDonald*, 1975; *Brennand*, 1994; *Benn and Evans*, 1998]. The nature of some eroding layers also suggests induration of the ridge sediments. Examples of cementation and/or induration have been observed in many locations on Mars [*Pain et al.*, 2007]. *Pain et al.* [2007] suggest that the most likely cementing agents for surface induration are iron oxides, silica, sulfates, and perhaps halide salts. Possible cementation mechanisms include evaporation, sublimation, surficial seepage or movement of moisture films [*Chavdarian and Sumner*, 2006; *Pain et al.*, 2007].

[38] Layers that extend into the surrounding topography along the west side of a portion of Cleia Dorsum (Figure 8a), may have formed owing to large cavities at the base of the ice; water flowing in a subice tunnel would also flow into other surrounding cavities beneath the ice forming similar layers to those deposited in the tunnel. Layers extending beyond the margins of the sinuous ridges may also represent an accumulation area at the edge of the ice that was just outside of the ice but continuous with features under the ice, potentially an ice marginal lake. Subglacial and ice marginal lakes and eskers are all commonly observed in terrestrial ice marginal environments and are commonly associated together. It should also be noted that the continuous layers are observed near the base of the sinuous ridge in this location and may have been emplaced in a depositional setting that existed at an earlier time, such as a preglacial lacustrine setting in the basin [e.g., *Parker*, 1989, 1994; *Kargel and Strom*, 1992; *Parker et al.*, 2000, 2003; *Kargel*, 2004]. In this scenario, once the lake froze or the area became covered with ice, the esker sediments would be deposited over the lacustrine sediments. Although the stratification observed in this area may not be typical of most terrestrial subglacial sediments, its formation is consistent with a glacial setting and does not conflict with the esker hypothesis.

[39] The occurrence of Argyre's ridges among layered deposits, and the crude parallelism of ridges with topographic contours allows for the possibility that lacustrine shore or near-shore processes were involved. Potentially, glacial/ice sheet esker deposition occurred penecontemporaneously, in the same large process system, with proglacial lacustrine and ice contact moraine depositional processes. In this context, sedimentary deposition occurred in interfingering and perhaps oscillating masses of ice, lake water, and glacial stream water in a manner similar to that which affected final major glacial depositional episodes involving the last lobes of decaying Pleistocene ice sheets (such as the Superior Lobe of the Laurentide Ice Sheet in northern Minnesota, and the Cordilleran Ice Sheet in central British Columbia). In such systems, moraines, eskers, kames, thermokarst, layered lake plains, and glaciolacustrine deltas overlap and interfinger in complex ice stagnation terrains; it is not always possible to isolate, with rigor and with idealized geomorphological definitions, one landform component from the others because they all are formed together as parts of the same large-scale process system.

5. Summary and Conclusions

[40] A suite of sinuous ridges with branching and braided morphologies forms an anastomosing network around the southern Argyre basin in the southern hemisphere of Mars. Past research has led to several proposed modes of origin for the ridges. Using HiRISE and CTX imagery and MOLA topographic data sets, we reexamine the characteristics of the ridges and reevaluate several proposed formation mechanisms. The map patterns and morphology of the ridges, their ability to cross topographic divides, their occurrence in troughs, the relationship of their height and crest shape to the slope of the surrounding surface, their location at >50°S latitude, and the occurrence of other possible glacial landforms in the surrounding region, indicate that the ridges are most likely eskers formed by glaciofluvial processes. The occurrence of Argyre's ridges among layered deposits allows for the possibility that lacustrine processes were involved. The nature of some eroding beds in the ridges suggests induration of ridge sediments. Alternating patterns of layers may also reflect the influence of cyclic fluctuations in meltwater and sediment availability. If the ridges were indeed formed by subice fluvial processes, this formation mechanism implies that the area of ridge exposure in southern Argyre was once covered by the margin of a large, thick, ice deposit that was stagnating or retreating, extended for hundreds of kilometers within the basin, and reached at least ~52°S latitude. During the period of ridge formation, water flowed on top, within, or beneath the ice deposit; the continuity and preservation of the ridges suggests that flow was primarily at the base of the ice. The size (up to hundreds of meters tall and several kilometers wide), aspect ratio, and extent (hundreds of kilometers) of the ridges, as well as preliminary calculations of discharge (lower limit on the order of $\sim 10^4$ m^3/s), suggest that a significant amount of water was available.

[41] **Acknowledgments.** We gratefully acknowledge the invaluable assistance of the entire HiRISE team, including the software developers, the uplink and downlink teams, and the science team. We would also like to thank H. J. Melosh, W. L. Jaeger, S. Byrne, V. C. Gulick, R. M. E. Williams, N. Schofield, S. Valesco, J. Wilfore, J. Sano, and C. M. Dundas for their comments, suggestions, and encouragement and S. Mattson, who produced the DEM used in this study. This paper also benefited from

detailed reviews by J. W. Head and an anonymous reviewer. This work was supported by the NASA Mars Reconnaissance Orbiter project managed through the California Institute of Technology's Jet Propulsion Laboratory.

References

Baker, V. R. (2001), Water and the Martian landscape, *Nature*, *412*, 228–236, doi:10.1038/35084172.

Banks, M. E. (2009), Glacial processes and morphologies in the southern hemisphere of Mars, Ph.D. dissertation, 216 pp., Univ. of Ariz., Tucson.

Banks, M. E., A. S. McEwen, M. T. Mellon, J. S. Kargel, V. C. Gulick, W. L. Jaeger, L. Keszthelyi, K. E. Herkenhoff, and the HiRISE Team (2007), Glacial morphologies in the western Charitum Montes, Argyre basin rim, *Lunar Planet. Sci.* [CD-ROM], *XXXVIII*, Abstract 2164.

Banks, M. E., et al. (2008), High Resolution Imaging Science Experiment (HiRISE) observations of glacial and periglacial morphologies in the circum-Argyre Planitia highlands, Mars, *J. Geophys. Res.*, *113*, E12015, doi:10.1029/2007JE002994.

Bannerjee, I., and B. C. McDonald (1975), Nature of esker sedimentation, in *Glaviofluvial and Glaciolacustrine Sedimentation*, edited by A. V. Jopling and B. C. McDonald, *Spec. Publ. Soc. Econ. Palentol. Mineral.*, *23*, 132–154.

Benn, D., and D. Evans (1998), *Glaciers and Glaciation*, 734 pp., John Wiley, New York.

Brennand, T. A. (1994), Macroforms, large bedforms and rhythmic sedimentary sequences in subglacial eskers, south-central Ontario: Implications for esker genesis and meltwater regime, *Sediment. Geol.*, *91*, 9–55, doi:10.1016/0037-0738(94)90122-8.

Brennand, T. A. (2000), Deglacial meltwater drainage and glaciodynamics: Inferences from Laurentide eskers, Canada, *Geomorphology*, *32*, 263–293, doi:10.1016/S0169-555X(99)00100-2.

Carr, M. H., and N. Evans (1980), *Images of Mars: The Viking Extended Mission*, U.S. Govt. Print. Off., Washington, D. C.

Chavdarian, G. V., and D. Y. Sumner (2006), Cracks and fins in sulfate sand: Evidence for recent mineral-atmospheric water cycling in Meridiani Planum outcrops?, *Geology*, *34*, 229–232, doi:10.1130/G22101.1.

Easterbrook, D. J. (1999), *Surface Processes and Landforms*, 352 pp., Prentice Hall, Upper Saddle River, N. J.

Forbes, D. L., and R. B. Taylor (1994), Ice in the shore zone and the geomorphology of cold coasts, *Prog. Phys. Geogr.*, *18*(1), 59–89, doi:10.1177/030913339401800104.

Ghatan, G. J., and J. W. Head (2004), Regional drainage of meltwater beneath a Hesperian-aged south circumpolar ice sheet on Mars, *J. Geophys. Res.*, *109*, E07006, doi:10.1029/2003JE002196.

Golombek, M. P., J. B. Plescia, and B. J. Franklin (1991), Faulting and folding in the formation of planetary wrinkle ridges, *Proc. Lunar Planet. Sci. Conf.*, *21st*, 679–693.

Golombek, M. P., F. S. Anderson, and M. T. Zuber (2000), Martian wrinkle ridges topography: Evidence for subsurface faults from MOLA, *Lunar Planet. Sci.*, [CD-ROM], *XXXI*, Abstract 1294.

Goulty, N. R., and N. Schofield (2008), Implications of simple flexure theory for the formation of saucer-shaped sills, *J. Struct. Geol.*, *30*, 812–817, doi:10.1016/j.jsg.2008.04.002.

Greeley, R., N. Lancaster, S. Lee, and P. Thomas (1992), Martian eolian processes, sediments, and features, in *Mars*, edited by H. H. Kieffer et al., pp. 730–766, Univ. of Ariz. Press, Tucson.

Grossenbacher, N., and S. M. McDuffie (1995), Conductive cooling of lava: Columnar joint diameter and stria width as functions of cooling rate and thermal gradient, *J. Volcanol. Geotherm. Res.*, *69*(1–2), 95–103, doi:10.1016/0377-0273(95)00032-1.

Head, J. W., III (2000a), Tests for ancient polar deposits on Mars: Origin of esker-like sinuous ridges (Dorsa Argentea) using MOLA data, *Lunar Planet. Sci.*, [CD-ROM], *XXXI*, Abstract 1116.

Head, J. W., III (2000b), Tests for ancient polar deposits on Mars: Morphology and topographic relationships of esker-like sinuous ridges (Dorsa Argentea) using MOLA data, *Lunar Planet. Sci.*, [CD-ROM], *XXXI*, Abstract 1117.

Head, J. W., III (2000c), Extensive south polar ice cap in middle Mars history?: Tests using MOLA data, *Lunar Planet. Sci.*, [CD-ROM], *XXXI*, Abstract 1119.

Head, J. W., and B. Hallet (2001a), Origin of sinuous ridges in the Dorsa Argentea Formation: Additional criteria for tests of the esker hypothesis, *Lunar Planet. Sci.*, [CD-ROM], *XXXII*, Abstract 1366.

Head, J. W., and B. Hallet (2001b), Origin of sinuous ridges in the Dorsa Argentea Formation: New observations and tests of the esker hypothesis, *Lunar Planet. Sci.*, [CD-ROM], *XXXII*, Abstract 1373.

Head, J. W., and S. Pratt (2001), Extensive Hesperian-aged south polar ice sheet on Mars: Evidence for massive melting and retreat, and lateral flow and ponding of meltwater, *J. Geophys. Res.*, *106*, 12,275–12,299, doi:10.1029/2000JE001359.

Head, J. W., III, et al. (2005), Tropical to mid-latitude snow and ice accumulation, flow and glaciation on Mars, *Nature*, *434*, 346–351, doi:10.1038/nature03359.

Head, J. W., L. Wilson, J. L. Dickson, and G. Neukum (2006), The Huygens-Hellas giant dike system on Mars: Implications for Late Noachian-Early Hesperian volcanic resurfacing and climatic evolution, *Geology*, *34*, 285–288, doi:10.1130/G22163.1.

Hiesinger, H., and J. W. Head (2002), Topography and morphology of the Argyre basin, Mars: Implications for its geologic and hydrologic history, *Planet. Space Sci.*, *50*, 939–981, doi:10.1016/S0032-0633(02)00054-5.

Hodges, C.A. (1980), Geologic map of the Argyre quadrangle of Mars, *U.S. Geol. Surv. Misc. Invest. Map.*, *I-1181(MC-26)*.

Holt, J. W., et al. (2008), Radar sounding evidence for buried glaciers in the southern mid-latitudes of Mars, *Science*, *322*, 1235–1238, doi:10.1126/science.1164246.

Hooke, R. L. (2005), *Principles of Glacier Mechanics*, Cambridge Univ. Press, Cambridge, U. K.

Howard, A. D. (1981), Etched plains and braided ridges of the south polar region of Mars: Features produced by melting of ground ice?, in *Reports of Planetary Geology Program-1981*, *NASA Tech. Memo 84211*, 286–289.

Huddart, D., M. R. Bennett, and N. F. Glasser (1999), Morphology and sedimentology of a high-arctic esker system: Vegbreen, Svalbard, *Boreas*, *28*, 253–273, doi:10.1080/030094899750044350.

Jackson, G. R. (1995), Flow velocity estimation of meltwater streams in subglacial conduits: A palaeohydraulic analysis of the Bridgenorth Esker, Peterborough County, Ontario, Honors thesis, Trent Univ., Peterborough, Ont., Canada.

Jöns, H.-P. (1987), Large fossil mud lakes or giant mud sheet floods in Syrtis Major (Isidis Planitia) and Mare Australe, *Lunar Planet. Sci.*, *XVIII*, 470–471.

Jöns, H.-P. (1992), Fossil glaciation in the environs of the south pole, Mars?, *Lunar Planet. Sci.*, *XXIII*, 633–634.

Jöns, H.-P. (1999), What happened really in Argyre Planitia, Mars?, paper presented at 24th Meeting, Eur. Geophys. Soc., The Hague, Netherlands.

Kargel, J. S. (1993), Geomorphic processes in the Argyre-Dorsa Argentea region of Mars, *Proc. Lunar Planet. Sci. Conf.*, *24th*, 753–754.

Kargel, J. S. (2004), *Mars: A Warmer Wetter Planet*, 550 pp., Springer, Chichester, U. K.

Kargel, J. S., and G. Strom (1992), Ancient glaciation on Mars, *Geology*, *20*, 3–7, doi:10.1130/0091-7613(1992)020<0003:AGOM>2.3.CO;2.

Kargel, J. S., V. R. Baker, J. E. Begét, J. F. Lockwood, T. L. Péwé, J. S. Shaw, and R. G. Strom (1995), Evidence of ancient continental glaciation in the Martian northern plains, *J. Geophys. Res.*, *100*, 5351–5368, doi:10.1029/94JE02447.

Kirk, R. L., et al. (2008), Ultrahigh resolution topographic mapping of Mars with MRO HiRISE stereo images: Meter-scale slopes of candidate Phoenix landing sites, *J. Geophys. Res.*, *113*, E00A24, doi:10.1029/2007JE003000.

Komar, P. D. (1979), Comparisons of the hydraulics of water flows in Martian outflow channels with flows of similar scale on earth, *Icarus*, *37*, 156–181, doi:10.1016/0019-1035(79)90123-4.

Lang, N. P. (2007), Sinuous ridge formation in southeastern Argyre Planitia, Mars, *Lunar Planet. Sci.*, [CD-ROM], *XXXVIII*, Abstract 1116.

Leopold, L. B., W. G. Wolman, and J. P. Miller (1964), *Fluvial Processes in Geomorphology*, Freeman, San Francisco, Calif.

Lorang, M. S., and F. R. Hauer (2003), Flow competence and streambed stability: An evaluation of technique and application, *J. North Am. Benthol. Soc.*, *22*(4), 475–491, doi:10.2307/1468347.

Mabbutt, J. A., and M. F. Sullivan (1968), The formation of longitudinal dunes: Evidence form the Simpson desert, *Aust. Geogr.*, *10*, 483–487, doi:10.1080/00049186808702520.

Mainguet, M. (1984), A classification of dunes based on eolian dynamics and the sand budget, in *Deserts and Arid Lands*, edited by F. El-Baz, pp. 31–58, Nijhoff, The Hague, Netherlands.

Mangold, N. (2000), Giant paleo-eskers of Mauritania: Analogs for Martian esker-like landforms, paper presented at Second International Conference on Mars Polar Science and Exploration, Abstract 4031, Lunar Planet. Inst., Reykjavík.

Mangold, N. (2003), Geomorphic analysis of lobate debris aprons on Mars at Mars Orbiter Camera scale: Evidence for ice sublimation initiated by fractures, *J. Geophys. Res.*, *108*(E4), 8021, doi:10.1029/2002JE001885.

Martini, I. P., M. E. Brookfield, and S. Sadura (2001), *Principles of Glacial Geomorphology and Geology*, Prentice-Hall, Upper Saddle River, N. J.

McEwen, A. S., et al. (2007), Mars Reconnaissance Orbiter's High Resolution Imaging Science Experiment (HiRISE), *J. Geophys. Res.*, *112*(E5), E05S02, doi:10.1029/2005JE002605.

Metzger, S. M. (1991), A survey of esker morphologies, the connection to New York state glaciation and criteria for subglacial melt-water channel deposits on the planet Mars, *Proc. Lunar Planet. Sci. Conf.*, *22nd*, 891–892.

Metzger, S. M. (1992), The eskers of New York state: Formation process implications and esker-like features on the planet Mars, *Proc. Lunar Planet. Sci. Conf.*, *23rd*, 901–902.

Metzger, S. M. (2002), Paleodischarge modeling of the Argyre ridge esker model, *Lunar Planet. Sci.*, [CD-ROM], *XXXIII*, Abstract 2045.

Miller, M. C., and P. D. Komar (1977), The development of sediment threshold curves for unusual environments (Mars) and for inadequately studied materials (Foram sands), *Sedimentology*, *24*, 709–721, doi:10.1111/j.1365-3091.1977.tb00266.x.

Pain, C. F., J. D. A. Clarke, and M. Thomas (2007), Inversion of relief on Mars, *Icarus*, *190*, 478–491, doi:10.1016/j.icarus.2007.03.017.

Parker, T. J. (1989), Channels and valley networks associated with Argyre Planitia, Mars, *Proc. Lunar Planet. Sci. Conf.*, *20th*, 826–827.

Parker, T. J. (1994), Martian paleolakes and oceans, Ph.D. dissertation, 200 pp., Univ. of South. Calif., Los Angeles.

Parker, T. J. (1996a), Highlights from 1:500K geologic mapping of central and southern Argyre Planitia, *Proc. Lunar Planet. Sci. Conf.*, *27th*, 1003–1004.

Parker, T. J. (1996b), The rich geomorphic legacy of the Argyre basin: A Martian hydrologic saga, in *Workshop on Evolution of Martian Volatiles*, *Tech. Rep. 96–01*, part I, pp. 36–37, Lunar Planet. Inst., Houston, Tex.

Parker, T. J., and D. S. Gorsline (1992), Preliminary geologic mapping of the MTM –55036 and -55043 quadrangles, southern Argyre Planitia, Mars, *Proc. Lunar Planet. Sci. Conf.*, *28th*, 1031–1032.

Parker, T. J., D. C. Pieri, and R. S. Saunders (1986), Morphology and distribution of sinuous ridges in central and southern Argyre: Reports of the planetary geology and geophysics program, *NASA Tech. Memo.*, *88383*, 468–470.

Parker, T. J., S. M. Clifford, and W. B. Banerdt (2000), Argyre Planitia and the Mars global hydrologic cycle, *Lunar Planet. Sci.*, [CD-ROM], *XXXI*, Abstract 2033.

Parker, T. J., J. A. Grant, F. S. Anderson, and W. B. Banerdt (2003), From the south pole to the northern plains: The Argyre Planitia story, in *Sixth International Conference on Mars, July 20–25, 2003, Pasadena CA* [CD-ROM], *LPI Contrib.*, *1164*, Abstract 3274.

Pollard, D. (1987), Elementary fracture mechanics pplied to the structural interpretation of dykes, in *Mafic Dyke Swarms*, edited by C. H. Hallsand and W. F. Fahrig, *Geol. Assoc. Can. Spec. Pap.*, *34*, 5–24.

Ritter, D. F., R. C. Kochel, and J. R. Miller (2002), *Process Geomorphology*, 734 pp., Waveland, Long Grove, Ill.

Röthlisberger, H. (1972), Water pressure in intra- and subglacial channels, *J. Glaciol.*, *11*, 177–203.

Ruff, S. W. (1992), Dorsa Argentea type sinuous ridges, Mars: Evidence for linear dune hypothesis, *Proc. Lunar Planet. Sci. Conf.*, *23rd*, 1171–1172.

Ruff, S. W., and R. Greeley (1990), Sinuous ridges of the south polar region, Mars: Possible origins, *Proc. Lunar Planet. Sci. Conf.*, *21st*, 1047–1048.

Scott, D. H., and K. L. Tanaka (1986), Geologic map of the western equatorial region of Mars, *U.S. Geol. Surv. Misc. Invest. Map I-1802-A*.

Shreve, R. L. (1985), Esker characteristics in terms of glacier physics, Katahdin esker system, Maine, *Geol. Soc. Am. Bull.*, *96*, 639–646, doi:10.1130/0016-7606(1985)96<639:ECITOG>2.0.CO;2.

Smith, D. E., et al. (2001), Mars Orbiter Laser Altimeter: Experiment summary after the first year of global mapping of Mars, *J. Geophys. Res.*, *106*, 23,689–23,722, doi:10.1029/2000JE001364.

Tanaka, K. L., and D. H. Scott (1987), Geologic map of the polar regions of Mars, *U.S. Geol. Surv. Misc. Invest. Map*, *I-1802-C*.

Theilig, E. E. (1986), Formation of pressure ridges and emplacement of compound basaltic lava flows, Ph.D. thesis, Ariz. State Univ., Tempe.

Wentworth, C. K. (1922), A scale of grade and class terms for clastic sediments, *J. Geol.*, *30*, 377–392.

Zuber, M. T., et al. (2000), Internal structure and early thermal evolution of Mars from Mars Global Surveyor topography and gravity, *Science*, *287*, 1788–1793, doi:10.1126/science.287.5459.1788.

M. E. Banks and J. D. Pelletier, Department of Geosciences, University of Arizona, Tucson, AZ 85721, USA.

V. R. Baker and J. S. Kargel, Department of Hydrology and Water Resources, University of Arizona, Tucson, AZ 85721, USA.

J. A. Grant, Center for Earth and Planetary Studies, National Air and Space Museum, Smithsonian Institution, Washington, DC 20013, USA.

N. P. Lang, Department of Geology, Mercyhurst College, Erie, PA 16546, USA.

A. S. McEwen and R. G. Strom, Lunar and Planetary Laboratory, University of Arizona, Tucson, AZ 85721, USA.